Swansea University
Prifysgol Abertawe

Statement Concerning
RACHMAD IRWANTO
Student Number: 501961 (**D.O.B.** 26/07/1980)

This is to certify that RACHMAD IRWANTO has been enrolled continuing as a writing up student of this University during the Session 09/10, pursuing a programme of study in Civil Engineering, leading to the degree of MSc of the University of Wales.

MR IRWANTO submitted a dissertation on15/10/2009 of which the result is pending

MR IRWANTO will be admitted to the degree 'in absentia' within three months of the result of the degree being confirmed and will be invited to attend a ceremony and celebrate his award the following July.

H.D.L. Morris
Academic Registrar

Official Stamp

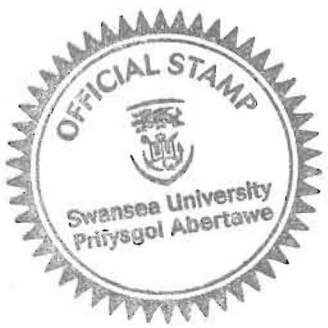

Invalid without stamp

THIS DOCUMENT IS ISSUED BY THE ACADEMIC REGISTRY AND BEARS NO MARKS
THIS DOCUMENT IS INVALID IF AMENDED IN ANY WAY

Our Ref: HLM/CP

Wednesday, 28 October 2009

Y Gofrestrfa Academaidd • Academic Registry
Parc Singleton, Abertawe, SA2 8PP, Cymru, DU • Singleton Park, Swansea, SA2 8PP, Wales, UK
Tel/Ffôn: +44 (0)1792 513546 Fax/Ffacs: +44 (0)1792 295157

SWANSEA UNIVERSITY HIGHER DEGREES SUBMISSION OF THESIS/DISSERTATION

RECEIPT FORM FOR THE SUBMISSION OF A DISSERTATION OR THESIS FOR THE DEGREE OF:

Master of Science
Civil Engineering

Student Reference Number : **501961/1**

Candidate's full name: **Rachmad Irwanto**

In the Department/ School of: **Engineering**

Dissertation / Thesis title: **An Impes Method for two-phase flow reservoir simulation**

Submission date: 15 October 2009

Student contact address for correspondence: **AL MAJAZ, SHARJAH**
P O BOX 72231
SHARJAH
UNITED ARAB EMIRATES

Financial Clearance: **Yes**

Regulatory Clearance: **Yes**

Matriculation: **Other Matriculated**

Please note that the University will not be able to complete the examination process fully until the student has enrolled, fulfilled his/her financial obligations to the University and has matriculated according to the regulations. Therefore if the student has not met all of these requirements he/she should visit / contact the Academic Registry in Singleton Abbey or the Finance Department (as appropriate).

Date: **Thursday, October 15 2009** Produced by y.m.rees

Copy for : **Student**

Thursday, October 15 2009

An IMPES METHOD FOR TWO-PHASE FLOW RESERVOIR SIMULATION

A THESIS
SUBMITTED TO THE SCHOOL OF ENGINEERING OF
SWANSEA UNIVERSITY
IN FULFILLMENT OF THE REQUIREMENTS
FOR THE DEGREE OF
MASTER OF SCIENCE

By

Rachmad Irwanto
501961

Swansea University
Prifysgol Abertawe

Swansea University
October 2009

Acknowledgements

The author is grateful to many individuals for their assistance and contribution for the accomplishing of this work. I wish to thank Professor Michael G. Edwards for his regular assistance and useful resources during the completion of this thesis. I also wish to acknowledge Dr. Robert Xiao for encouraging me to undertake this topic for my thesis.

I also wish to thank my colleagues who have supported me to finish the work with their hand-out notes and also MATLAB® Central (online user community) for the useful examples.

Finally, my acknowledgement is for my families who have been unfailing support for me all the time.

Rachmad Irwanto

Swansea, October 2009

Declaration

This work has not previously been accepted in substance for any degree and is not being concurrently submitted in candidature for any other degree.

Signed .....(candidate)

Date .....

Statement 1

This thesis is the result of my own investigations, except where otherwise stated.

Other sources are acknowledged by footnotes giving explicit references. A bibliography is appended.

Signed .....(candidate)

Date .....

Statement 2

I hereby give consent for my thesis, if accepted, to be available for photocopying and for inter-library loan, and for the title and summary to be made available to outside organisations.

Signed .....(candidate)

Date .....

Abstract

An introduction of reservoir modeling is a useful knowledge for structural engineers to extend their job opportunity. This thesis presents discretisation of fluid flow equations inside reservoir in simplistic models and visualizes into some graphical profiles. We start with Darcy's equation and mass continuity equation to derive pressure equation for single-phase flow through finite difference approximation. We then carry on multi-phase flow derivation under IMPES method, which involves relative permeability function inside saturation solver. Multi-phase flow that we present is water-oil system in 2D areal model. Later we disclose the effect of mobility ratio on oil displacement efficiency through Buckley-Leverett solution. The solution defines the position of fluid front against time during water-flooding process. We also present some flow profiles of the existence of barriers inside reservoir. This attempt is meant to close the real heterogenic condition of reservoir. For result comparison, we also review some methods of the implementation of higher order finite element for flow approximation.

Contents

Figure List

Nomenclature

Latin

A	area
a	transmissibility matrix
f_w	water fractional flow
$f(S)$	fractional flow as a saturation function
g	gravity
h	height
K, k_{abs}	rock permeability
$\frac{K}{\mu} x$	mobility in x-axis
$\frac{K}{\mu} y$	mobility in y-axis
k_{eff}	fluid phase permeability in multi-phase flow
k_{rw}	water relative permeability
k_{ro}	oil relative permeability
L	length
N	number of grids
p	pressure
p_c	capillary pressure
p_o	oil pressure
p_w	water pressure
Q, q	sink/source points (production per unit time)
S	saturation
S_o	oil saturation
S_w	water saturation
S_{or}	oil residual saturation
S_{wc}	water residual saturation
T	transmissibility matrix
t	time
U, u	pressure
V, v	mass velocity rate (unless differently specified)
x, y, z	distance at Cartesian axis

Greek

λ	mobility
λx	mobility in x-axis
λy	mobility in y-axis
μ	viscosity
ρ	mass rate
ϕ	rock porosity
Δt	difference for time derivative
∂	partial difference
$\overline{\Lambda}$	$\overline{\Lambda} = (\lambda_w \rho_w + \lambda_o \rho_o)$.
Ω	reservoir boundary

Superscript/Subscript

i	unit vector along x-axis
j	unit vector along y-axis
n	iteration at n^{th}
o	oil phase
w	water phase
x, y, z	directions in Cartesian axis
T	total

Operator

∇	gradient
∇^2	Laplacian
$\nabla.$	divergence

1 Introduction

1. Introduction

Today structural engineers are mainly assigned for structural facilities project with straight dependency on global financial condition of the region. This is because construction industry is generally long-term needs of people. In the other hand, mining industry or more specifically petroleum industry in which civil engineers are mostly dispossessed seems to be more stable since the product is people's daily consumption and generally leave the reliance stability to international political condition. Later chapters will show that any engineering disciplines with numerical analysis background may learn and take part in petroleum industry. However, a meticulous interpretation in every subject may still require ones who understand mathematical analysis and philosophy of the subject.

One of disciplines in petroleum industry is reservoir engineering which strongly related with other engineering discipline through numerical solution in fluid mechanics. Reservoir engineering is basically an engineering discipline that deals with a task of how to acquire oil inside a reservoir. The reservoir is normally multi-layers of permeable rock that located deep inside the earth surface. In other word, the simulation model is based on the understanding of fluid flow in porous media[1]. Reservoir modelling, more specifically, is an intersecting point of some other disciplines. To mention some disciplines that contribute to reservoir engineering are fluid dynamics, petrophysics, grid generation, seismic interpretation, geological modelling, and other data interpretations. Reservoir simulation allows us to gain better insight of petroleum recovery mechanism[2].

[1] Source: [1]
[2] Source: [1]

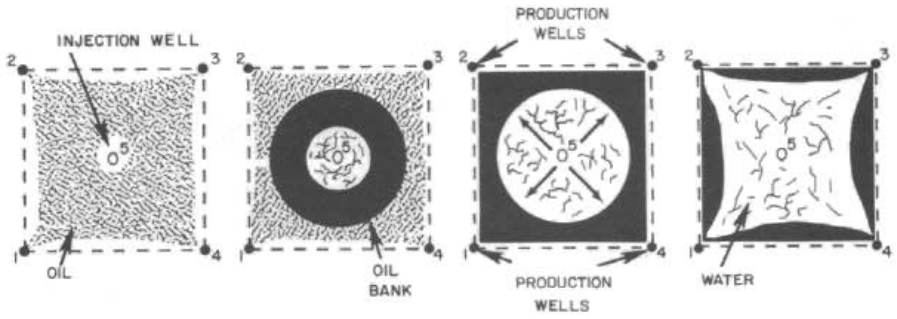

Figure 1. A five spot pattern of reservoir model.[3]

We, in this book, adjusting with the provided time to accomplish this book, try to develop a simple model of flow inside reservoir. Since it is a simple model, any advance heterogeneous rock properties (e.g. rock fractures) are neglected. Generating a reservoir model with simple finite difference discretisation is one way to start understanding the reservoir recovery mechanism. Through MATLAB®, we visualize our first finite difference discretisation on single-phase flow to solve pressure equation derived from Darcy's velocity and mass conservation equations.

Involving some more properties such porosity, viscosity, relative permeability and saturation, we then develop the discretisation on two-phase flow under water-oil system. As mentioned in the name, we use two-phase flow model which is the fluids are immiscible to each other. Unlike miscible flow (e.g. gas-oil system) where gas here will come out with oil together at the outlet, in the other hand, water here will push the oil to the outlet. Therefore, we can expect that the oil produced at the outlet is water-free, until the breakthrough time when water has reached the last grid block. Under two-phase flow condition, we use IMPES method to solve the equations that consists of pressure and saturation solvers. We also include some analysis of alternative implementation of higher order finite element for grid analysis in solving pressure equation. Other papers we will review later, result the use of control volume distributed (CVD) indicating the improvement of fluid front profile in two-phase flow. These methods are solutions to cope with non-uniform grids in reservoir discretisation.

Under IMPES, the approximation is a time function discretisation that involves some variables such Courant restriction for time step and Bukley-Leverett solution for oil displacement analysis. In particular, Courant restriction or known as CFL number, will give us insight of the saturation profile at any time step between $\Delta t = 0$ and $\Delta t = 1$. Further will also present that typically the homogenous areal model fluid breakthrough

[3] Source: [9]

takes place when the injected water has fulfilled 0.6 – 0.7 pore volume of the reservoir. Buckley-Leverett equation will provide us with equation to define the position of fluid front at time Δt. From this stage, we will notice the role of mobility ratio to the displacement efficiency.

In the real condition, reservoir is normally not as simple as we model. Some barriers may exist inside. The barriers physically exist as impermeable rock layer or the one with close to zero-permeability. In this book, we also try to visualize the flow profiles with the existence of barriers.

1.1 Study Objectives

Introductory to basic analysis of reservoir modelling is of our primary reasons for developing this report. Our main professional background is civil-structural engineering. We dealt with axial element analysis and its structural behaviour under dynamic forces with finite element-based packages. It helps to understand some basic numerical analysis required to develop MATLAB® coding for reservoir discretisation in this report. We realize that this discipline requires optimization more than what we used to carry on in practical construction industry. Nevertheless, we hope these basic understandings of reservoir modelling may lead to wider professional job opportunity and foundation of further study in this particular discipline.

In more specific objectives, we expect to achieve some points we mentioned above. Summarizing the discussion, the points we expect to achieve are listed below.

1. To discretise pressure profile of single flow through 2D areal grid-blocks from Darcy's equation and mass conservation law with finite difference approximation.
2. To discretise governing equations for two-phase immiscible fluid flow in 2D areal grid-blocks with IMPES method.
3. To profile the discretisation of the equations (single-phase flow and two-phase flow) through MATLAB® coding.
4. To visualize pressure, relative permeability, fractional flow, and saturation profile of the flow.
5. To review the implementation of higher order finite element method as the solution for flux approximation on unstructured grid in reservoir modelling.

2 Single-Phase Flow

2. Single-Phase Flow

2.1 Constructing uniform grids in 2-D

The first step for discretising the model is constructing grids. There are two model types in 2D Cartesian grids. 2D cross-sectional (x/z) grids may be used to study vertical sweep efficiency in a heterogeneous layered system, calculate water-oil displacement in a cross-section with geostatistic features, generate pseudo-relative permeabilites, study the mechanism of a gas displacement process to determine the importance of gravity etc. The second type is 2D areal (x/y) grids may be used to calculate areal sweep efficiencies in a water-flood or a gas flood, examine the stability of a near-miscible gas injection within a heterogeneous reservoir layer; examine the benefits of infill drilling in an areal pattern flood etc.

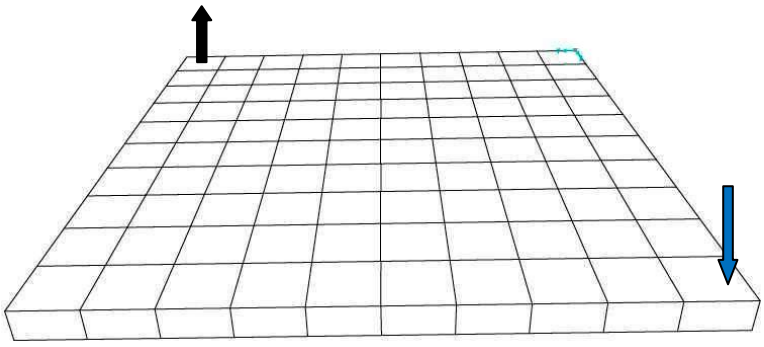

Figure 2. Areal 2D model with an injector and a producer.

In this section, to emphasize the effect of well pattern and assuming that there will be very little vertical movement, we use finite difference point distributed grids in areal model. From the point distributed grids method, we have $\Delta x = L/(N-1)$, where the first and the nth points will be at $x=0$ and $x=L$.

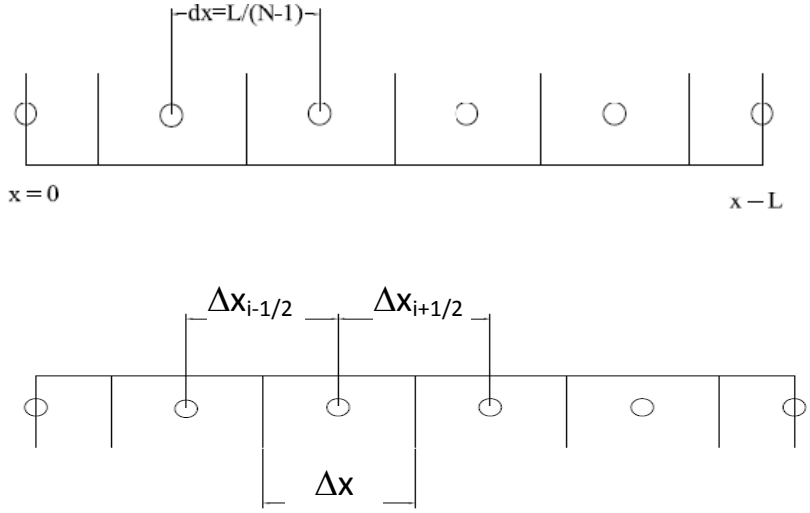

Figure 3. Point distributed grids

For the discretisation, normally it is assumed that rock properties such as permeability and porosity are assigned to grid blocks. The fluid transfers from one block to the rest of the whole reservoir through immediate neighbouring blocks. In 2D model, there will be four neighbouring blocks as figured below.

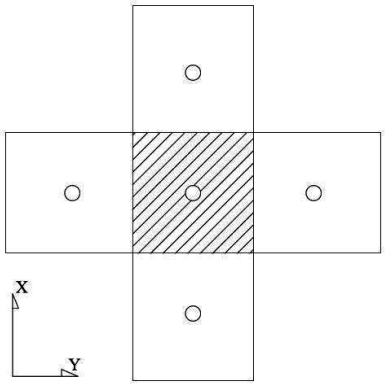

Figure 4. Neighbouring blocks in 2D model

2.2 Governing Equations for single flow

Similar to heat transfer equation, Darcy's main equation for fluid flow in porous media is proportional combination of fluid pressure and gravity in permeable layer. Flow equations from Darcy velocity state:

$$v = -\frac{K}{\mu}(\nabla p + \rho g \nabla h) \quad (1)$$

Here v is volumetric flow density and $\frac{K}{\mu}$ is permeability over viscosity (mobility of fluid) and p is pressure gradient. Normally K is a diagonal anisotropic tensor where in

2D flow, K_{11} and K_{22} are different value to each other. In matrix form, K will be $\begin{bmatrix} K_{11} & 0 \\ 0 & K_{22} \end{bmatrix}$

Permeability will run as harmonic average when the flow passes through heterogeneous layer while it may run as arithmetic average when the flow runs in parallel layer. For the model described later, we simply model the flow runs as harmonic average. In 2D single flow-areal model, considering $u=p - \rho gh$ we write the equation as follow.

$$v = -\frac{K}{\mu}(\nabla u) \tag{2}$$

The basic equation for the flow is also describing mass continuity. Adopted from mass conservation equation, we have:

$$-\nabla.\rho\, v = \frac{\partial}{\partial t}(\rho\phi) + q \tag{3}$$

We here will carry on deriving equations to approximate the pressure gradient of the flow, by combining equation (2) and equation (3).

$$\nabla.\rho\frac{K}{\mu_w}[\nabla u_w] = \frac{\partial}{\partial t}(\rho\phi) + q_w \tag{4}$$

Adopted from [1], conservation mass in equation (3) can also be generalised since$\rho\, v = m$, where m is mass component in unit volume and $\rho\, \phi\, S_l = m$ where S_l is saturation phase (later described in next sub chapter) and m is mass flux of phase l.

$$-\nabla.\rho\, v = \frac{\partial}{\partial t}(\rho\, \phi\, S_l) + q \tag{5}$$

2.3. Discretising single flow in finite difference form

For single flow, the approximation will neglect the time variable, therefore from equation (4) we have some main variables like $\frac{\partial p}{\partial x}$, $\frac{\partial^2 p}{\partial x^2}$ to be solved. In expanded term, we can re-write the variables as follows.

$$\frac{\partial p}{\partial x} = \frac{p_{i+1} - p_i}{\Delta x};$$

$$\frac{\partial^2 p}{\partial x^2} = \frac{\frac{p_{i+1} - p_i}{\Delta x} - \frac{p_i - p_{i-1}}{\Delta x}}{\Delta x}$$

The illustration of finite difference approximation is as figured at figure below. It must be kept that in doing finite difference approximation; Δx and Δy are maintained constant.

In this section, we carry on equation (4) to illustrate the flux flow. Let fluid mobility, $\lambda = {}^{K}/_{\mu}$. We then develop a statement as follow.

$$-\nabla.\ \lambda\,\nabla u = \frac{q}{\rho} \tag{6}$$

From grid discretisation above, it defines $\Delta x_{i-1/2}$ and $\Delta x_{i+1/2}$ that we will use for expanding equation (6) into 2D form. Since Δx and Δy are maintained constant, then we may assume $\Delta x_{i-1/2} = \Delta x_{i+1/2}$. We let each grid block has mobility λ_i and the fluid flow through grid perimeter which has mobility $\lambda_{i\pm1/2}$. Taking from equation (6), while keeping $\Delta z = 1$, we expand divergence and gradient operators form as follow;

$$\begin{aligned}-\nabla.\ \lambda\,\nabla u = {} & \frac{K}{\mu_w} x_{i+\frac{1}{2}}\left[\frac{u_{i+1,j}}{\Delta x^2} - \frac{u_{i,j}}{\Delta x^2}\right] + \frac{K}{\mu_w} x_{i-\frac{1}{2}}\left[\frac{u_{i-1,j}}{\Delta x^2} - \frac{u_{i,j}}{\Delta x^2}\right] \\ & + \frac{K}{\mu_w} y_{j+\frac{1}{2}}\left[\frac{u_{i,j+1}}{\Delta y^2} - \frac{u_{i,j}}{\Delta y^2}\right] + \frac{K}{\mu_w} y_{j-\frac{1}{2}}\left[\frac{u_{i,j-1}}{\Delta y^2} - \frac{u_{i,j}}{\Delta y^2}\right] \\ & = u_{i,j}^{n+1} - u_{i,j}^{n}\end{aligned} \tag{7}$$

Mobility λ as mentioned previously will run as harmonic average.

$$\lambda_{i+\frac{1}{2}} = \frac{\frac{\Delta x_i}{2} + \frac{\Delta x_{i+1}}{2}}{\frac{\Delta x_i}{2\ \lambda_i} + \frac{\Delta x_{i+1}}{2\ \lambda_{i+1}}}$$

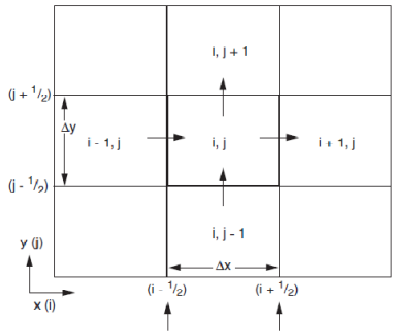

Figure 5. Block to block flow where the (i ± 1/2) and (j ± 1/2) subscripts refer to quantities at the boundaries.[4]

[4] Source: [4]

The way to identify the block position in numerical simulation is by block ordering. A particular ordering scheme may work specifically for particular simulation. This report uses natural ordering which gives a sequence order for the whole blocks assuming the reservoir as a rectangular block. In our MATLAB® coding, after setting up K matrix, grid block number and source/sink point, we then set the transmissibility as harmonic average before we construct the transmissibility matrix and solve the pressure equation. While solving the matrix we also set the prescribed pressure at grid (1, 1) equals to zero by adding element (1, 1) excluding itself to all the values in the first row and first column of permeability matrix.

In approximating the pressure with finite difference, the pressure in left hand side of the equation is pressure at *n+1*, and the pressure that we approximate in right hand side is pressure at *n* that in some points are assigned either as injectors or producers. We then carry on rearranging equation (6) above by grouping all unknown (pressure at n+1) to LHS and known terms to RHS.

$$-\left[\frac{\frac{K}{\mu_w}x_{i+\frac{1}{2}}}{\Delta x^2}\right]u_{i+1,j}^{n+1}-\left[\frac{\frac{K}{\mu_w}x_{i-\frac{1}{2}}}{\Delta x^2}\right]u_{i-1,j}^{n+1}+\left[\frac{\frac{K}{\mu_w}x_{i+\frac{1}{2}}}{\Delta x^2}+\frac{\frac{K}{\mu_w}x_{i-\frac{1}{2}}}{\Delta x^2}+\frac{\frac{K}{\mu_w}y_{j+\frac{1}{2}}}{\Delta y^2}+\frac{\frac{K}{\mu_w}y_{j-\frac{1}{2}}}{\Delta y^2}\right]u_{i,j}^{n+1}-\left[\frac{\frac{K}{\mu_w}y_{i-\frac{1}{2}}}{\Delta y^2}\right]u_{i,j-1}^{n+1}-\left[\frac{\frac{K}{\mu_w}y_{i+\frac{1}{2}}}{\Delta y^2}\right]u_{i,j+1}^{n+1}=u_{i,j}^{n} \quad (8)$$

In 2D, each block has five non-zero terms that constructs a penta-diagonal transmissibility matrix. Since the known terms in left hand side are constant, we then simplify equation (8) into:

$$a_{i+1}.u_{i+1,j}^{n+1}+a_{i-1}.u_{i-1,j}^{n+1}+a_{ij}.u_{i,j}^{n+1}+a_{j-1}.u_{i,j-1}^{n+1}+a_{j+1}.u_{i,j+1}^{n+1}=q.u_{i,j}^{n} \quad (9)$$

Even though we do not model in 3D, likewise, we may expand expression in equation (9) in 3D as below.

$$a_{i+1}.u_{i+1,j,k}^{n+1}+a_{i-1}.u_{i-1,j,k}^{n+1}+a_{ijk}.u_{i,j,k}^{n+1}+a_{j-1}.u_{i,j-1,k}^{n+1}+a_{j+1}.u_{i,j+1,k}^{n+1}+a_{k+1}.u_{i,j,k+1}^{n+1}+a_{k-1}.u_{i,j,k-1}^{n+1}=q.u_{i,j,k}^{n}$$

We then set boundary conditions for the whole inner blocks perimeter as flow boundary condition and outer blocks perimeter as no-flow boundary, therefore in perimeter along the reservoir $\partial\Omega$, we set $v_w .n = 0$, where n is normal vector pointing outward the boundary. Some points where we set as injector or producer wells as flow boundaries with pressure, therefore in the certain spots of reservoir $\partial\Omega$, we set $v_w .n = q$. Matrix q as sink/source point will be represented as 1 and -1. In 1D form, we simply set no flow boundary on top and bottom perimeter, sing point along the left perimeter and source point along the right perimeter. We then will end up with a simple matrix operation T * U = Q.

For example, in simple form of a 4x3 grid block with natural ordering block, the equation will appear as a sparse diagonal matrix below.

	1	2	3	4	5	6	7	8	9	10	11	12
1	x	x			x							
2	x	x	x			x						
3		x	x	x			x					
4			x	x				x				
5	x				x	x			X			
6		x			x	x	x			x		
7			x			x	x	x			x	
8				x			x	x				x
9					x				X	x		
10						x			X	x	x	
11							x			x	x	x
12								x			x	x

Figure 6. A natural 4 by 3 ordering block connectivity with its penta-diagonal non-zero transmissibility matrix.

The transmissibility matrix will have the same size for a 3x4 grid block. For the same ordering block, the different will be the position of transmissibility in *y*-direction.

It is essential to treat each reservoir block as a three-dimensional shape no matter we run the model in 1D, 2D, or 3D. Boundary conditions on each grid-blocks manage flow contribution the among the grid blocks. Specifically for this section, in 2D areal flow, two boundary conditions where we reckon as no flow boundary, do not contribute to flow. This explains the statement above why in 2D flow there are only four neighbouring blocks.

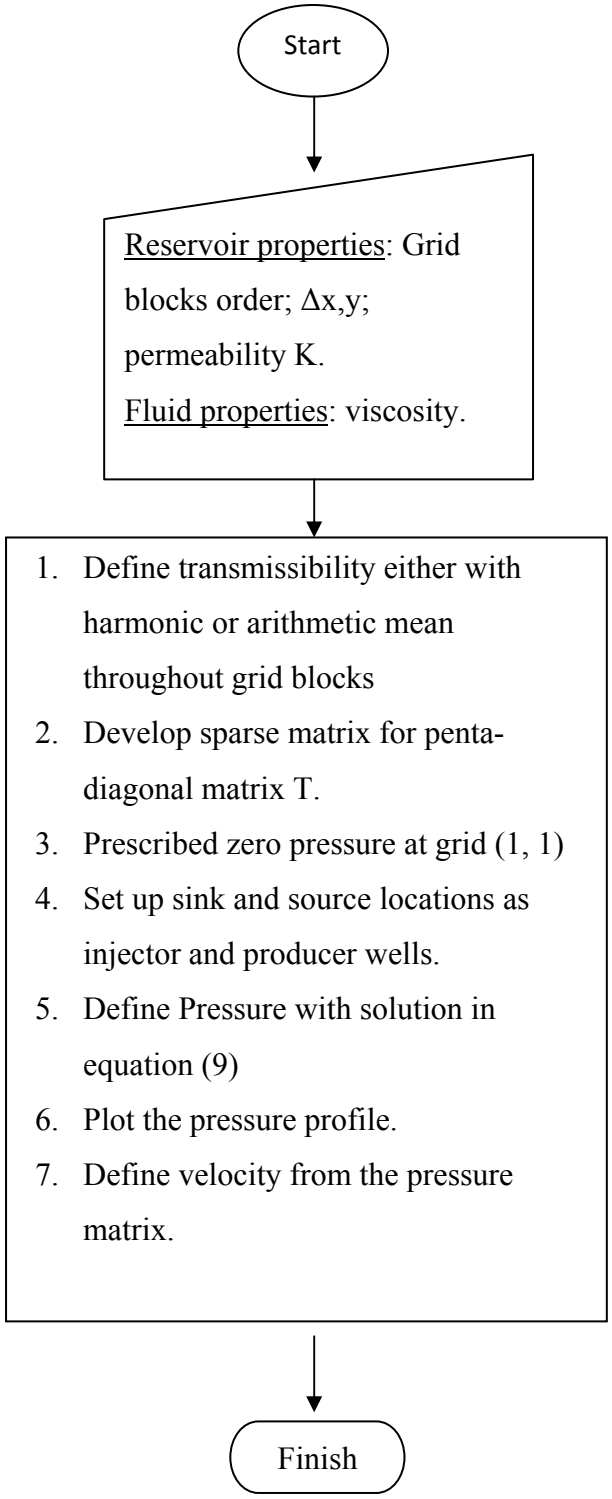

Figure 7. Flowchart for pressure solver.

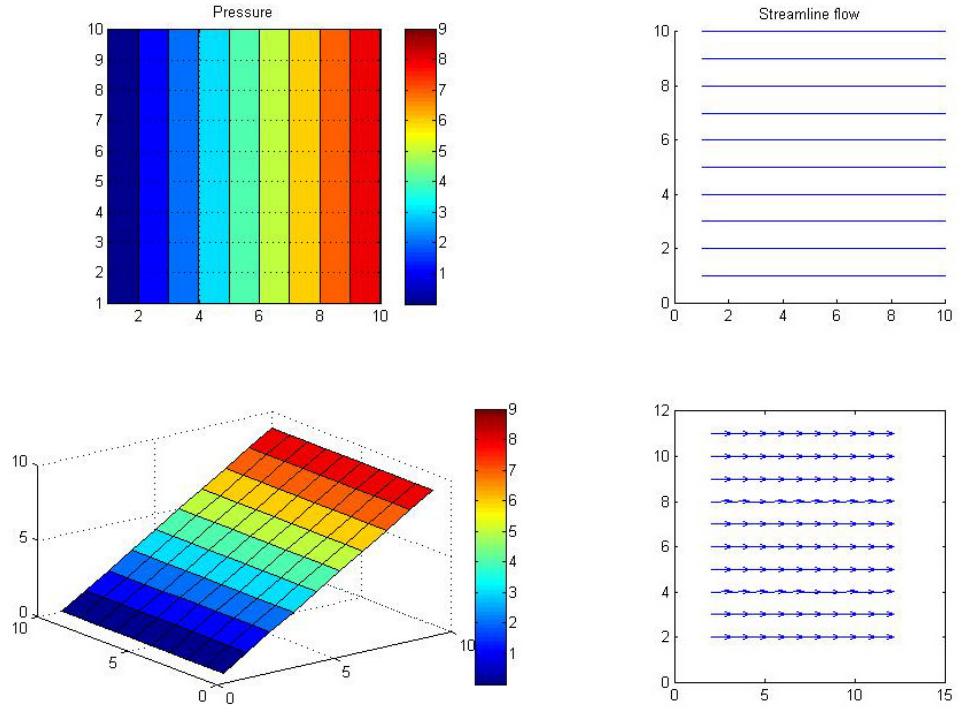

Figure 8. Pressure plot for 10 by 10 grid-blocks order in 1D.

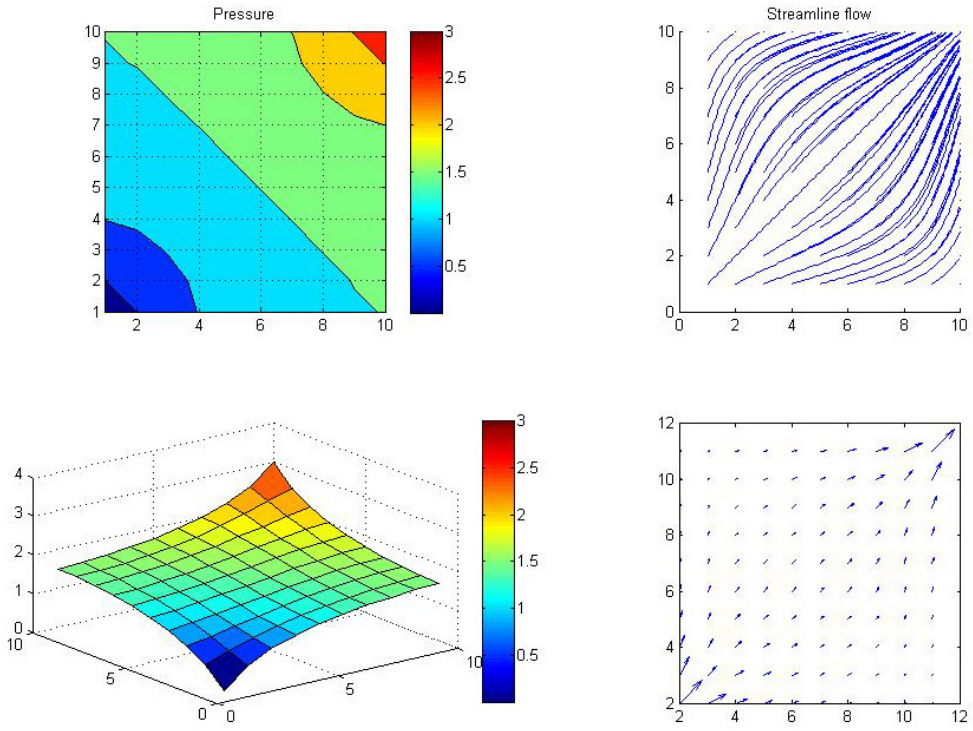

Figure 9. Pressure plot for 10 by 10 grid-blocks order in 2D.

2.4 Applicability of mixed FEM for pressure solver.

What we have presented above is a simple form of control volume finite element in 2D with finite difference approximation, where the space discretisation is kept constant. The method is useful to avoid complexity in the coupled system approximation. Some adaptive methods have been developed to account non-uniform grids in reservoir discretisation. Some papers and literatures are in detail discussing the application of mixed-FEM, such as [10], [11], and [12].

We will generally review the application of mixed-FEM. The method will approximate the flow as it transfers from one block to another through the grid edges. The transmissibility matrix will be bigger in size since it consists of edge transmissibilities associated with their length instead of block transmissibilities with constant length of space. This approximation allows the computation to have non-uniform grids. In multi-phase flow application, the pressure solver using Mixed-FEM may simply replace the one with finite difference approximation we have discretised above. This is because the input and the output variables for this method are the same with finite difference approximation.

2.4.1 Governing equations

The governing equation is taken from re-writing equation (2) and (6) with mixed-FEM. Defining Sobolev space, for $H^1(\Omega), v \in (L^2(\Omega)^2)$ and $\nabla . v \in L^2(\Omega)$.

$$-\nabla.(\lambda\, \nabla p) = q \quad x \in \Omega \text{ (Reservoir)} \tag{10}$$

$$v = -\lambda\, \nabla p \tag{11}$$

This method separates equation (11) where *v* is adopted from mass conservation law $\nabla . v = q$. The method is so called mixed method because the solution, instead of solving pressure and then sequentially using it to obtain velocity, it solves equation (11) and mass conservation equation for pressure and velocity at the same time. With no flow boundary condition and letting n is normal direction, it is set that $\nabla p . \mathrm{n} = 0$ at $x \in \partial\Omega$. Let *w* is a test function, we then multiply equation (11) with *w* and integrate it by part to obtain:

$$\int_\Omega \frac{v}{\lambda}\, w\, dx - \int_\Omega p\, \nabla . w\, dx = \int_\Omega \rho g . w\, dx \tag{12}$$

The method again sets another test function *l* and integrates over Ω, to have:

$$\int_{\Omega} l \nabla . v \, dx = \int_{\Omega} l \, q \, dx \tag{13}$$

Under simple control volume with finite difference approximation, *p* and *l* are set into piecewise constant. In matrix formational equation, we re-write equation (12) and (13) as follow.

$$\begin{bmatrix} B & -C^T \\ C & 0 \end{bmatrix} \begin{bmatrix} v \\ p \end{bmatrix} = \begin{bmatrix} \mathrm{g} \\ f \end{bmatrix}$$

In the matrix solution, [B] is the first term of left hand side in equation (12) consisting transmissibility over base function and [C] in the second term of left hand side of equation (12) stands for pressure over the base function. In the right hand side of matrix, we consider [g] is the right hand side expression of equation (12), for 2D areal model neglecting gravity the value will be zero. The location of sink/source is finally represented by matrix [*f*] whose values are 1 for producer, -1 for injector and zero for the rest, represents the right hand side of equation (13). Unknown [*p*] is the pressure matrix.

In 2D Raviart-Thomas element discretisation, the grid can be either rectangular or triangular. Under this approximation, we may come up with edge-based FEM. It is out of our scope to discuss more on mixed-FEM, however more details of mixed-FEM is discussed by *Wriggers and Carstensen* in [12].

3 Two-Phase Flow

3. Two-Phase Flow

3.1 Relative Permeability

Under two-phase flow condition, there would be displacing fluid and displaced fluid. It can be explained as one phase of fluid flow disturbs the existence of another fluid behavior.[5] In multi phase condition, we define $K_r = \frac{K_{eff}}{K_{abs}}$, where K_{eff} is fluid phase permeability. Later we will describe with a water-flooding illustration that under multi-phase condition, relative permeability is a function of saturation.

Our single-phase flow is weighted in harmonic means. Under multi phase flow, which involves two different phases, it cannot simply use the same averaging. As an illustration, we have two sequent blocks for two fluid phases (oil and water). In block *i* is at S_w, say only water can flow that means $k_{rw} > 0$ and $k_{ro} = 0$. Likewise for block *i+1*, say only oil can flow with $k_{rw} = 0$ and $k_{ro} > 0$. Physically we explain how water is the only fluid to be allowed to flow from block *i* to block *i+1*. We can say that equation (8) with harmonic average, at *i+1* for $k_{rw} = 0$ results in zero division which means it does not allow both water and oil to flow. Another averaging, that is arithmetic average as described below allows both water and oil to flow, which is incorrect according to the explanation above.

$$\lambda_{i+1/2} = \frac{\frac{\Delta x_i}{2}\,\lambda_{\mathrm{i}} + \frac{\Delta x_i}{2}\,\lambda_{\mathrm{i+1}}}{\frac{\Delta x_i}{2} + \frac{\Delta x_{i+1}}{2}}$$

A simple illustration of linear water-flooding is likely figured below. Each subfigure represents a time step, Δt, of the water injection process. An injector is located at block 1 is injecting water at constant rate V_w and a producing well is assigned at the 5th block. The system is initially set at saturation S_{wc} with no flow due to zero relative permeability of water $(k_{rw}(S_{wc}) = 0)$ at this particular stage. Each block has pore volume $Vp = \Delta x.A.\phi$, where ϕ is the cell porosity. At first time step, certain

[5] Source: [2]

volume of water is injected into block 1 as much as $V_w.\Delta t$ that would increase water saturation in block 1 into $S_{wc}=S_{wc}+(V_w.\Delta t)/Vp$. At this stage, no flow condition due to zero permeability is still maintained. The second time step, from injector at the first step, we keep injecting the same volume of water causing more increase in water saturation at block 1, since water saturation has changed, $k_{rw}(S_{w1}) > 0$, the new injected water will push the existing water inside the grid to flow from block 1 to block 2. Over the second stage, the flowing water from block 1 to block 2 will repeat the first condition which would increase water saturation at block 2 and if some more water at the next time step is injected, the condition would let water flow from block 2 to block 3, $k_{rw}(S_{w2}) > 0$. During this stage, the outlet is producing oil continuously. The same sequence occurs at the next time step then water will reach the last block with less rate of volume due to small relative permeability of water. Hence, for the time step, we notice that minimum number required is clearly associated with grid block number. Later explanation with Buckley-Leverett equation, we will describe this grid-based numerical dispersion may lead to numerical error approximation.

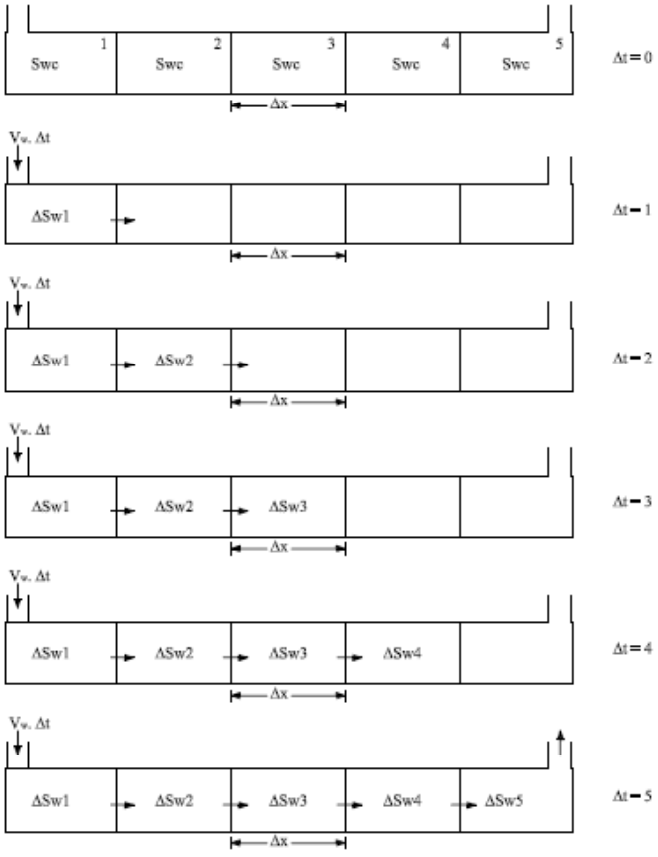

Figure 10. Numerical Dispersion illustration

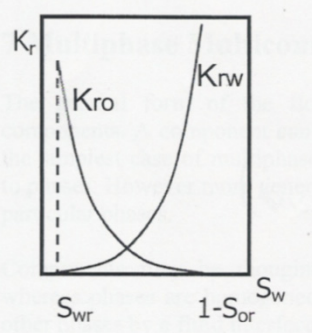

Figure 11. Relative permeability.[6]

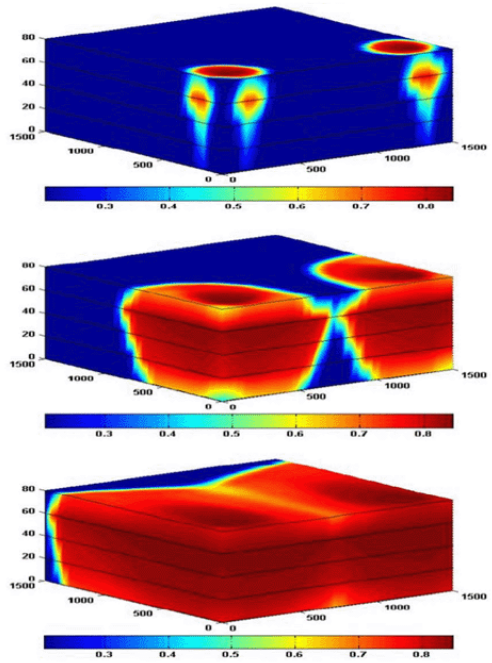

Figure 12. Water Saturation. These sample maps in sequence show the interval of 1.5 and 9 years in a reservoir model with two injectors.[7]

Mobility ratio in multi phase condition, based on the illustration above, can be defined as the ratio of the mobility of injected fluid behind the fluid front over mobility of another fluid. The first fluid in our model is water that is displacing the second one that is oil.

3.2. Equations for two-phase flow

There are basically two conceptual models for multi phase flow. The first one is two-phase model of two immiscible fluids. This model assumes that the phases are fully immiscible which means the soluble effect is neglected. The second model assumes that

[6] Source: [3]
[7] Source: [11]

each phase consists of two components and generally known as multi component flow. This presentation will focus on the first concept, which is two immiscible phases for water as displacing fluid and oil as displaced fluid. In many literatures, the phases in two-phase immiscible flow scheme are distinguished as wetting phase, which is normally water phase and non-wetting phase, which is the oil phase.

Taking statements from equation (2), (3), (4) and (5), the pressure equations for each phase are described below.

$$\nabla.\left[\lambda_o(S_o)[\nabla p_o]\right] = \phi\frac{\partial S_o}{\partial t} \quad \text{; for oil} \tag{14}$$

$$\nabla.\left[\lambda_w(S_w)[\nabla p_w]\right] = \phi\frac{\partial S_w}{\partial t} \quad \text{; for water} \tag{15}$$

$$\lambda_T(S_o) = \lambda_w(S_w) + \lambda_o(S_o) \tag{16}$$

Where λ_T is the total mobility. Other descriptions come along with the equations above are $S_o+S_w = 1$ and $p_o = p_c - p_w$, where p_c is capillary pressure. Equation (14), (15), (16) are rewriting the two-phase flow equation into

$$\nabla.\left[\lambda_T(S_o)[\nabla p]\right] = \phi\frac{\partial S_w}{\partial t} \tag{17}$$

For solving non-linearities in equation (17), we, first of all, define Darcy's phase velocity for each phase which is the basic equation to solve pressure solver. Taking from equation (1), we then define water velocity and oil velocity in full formational equation below.

$$V_w = -\lambda_w K(\nabla p_w + \rho_w g\nabla h) \tag{18}$$

$$V_o = -\lambda_o K(\nabla p_o + \rho_o g\nabla h) \tag{19}$$

To be noted, the gravity variable in the equations will further be neglected as we focus on areal model. Where total velocity $Vt = Vw + Vo$, taking from equation (18) and (19), we have:

$$\begin{aligned} V_T &= -\lambda_o K\,\nabla p_o - \lambda_w K\,\nabla p_w - (\lambda_w\rho_w + \lambda_o\rho_o)gK\,\nabla h) \\ &= -\lambda_o K\,\nabla(p_c - p_w) - \lambda_w K\,\nabla p_w - (\lambda_w\rho_w + \lambda_o\rho_o)gK\,\nabla h) \end{aligned} \tag{20}$$

To simplify the equation above, we let $\lambda_T = (\lambda_w + \lambda_o)$ and $\overline{\Lambda} = (\lambda_w\rho_w + \lambda_o\rho_o)$.

Substituting the assumptions into equation (20) then we have:

$$V_T = -\lambda_T K\,\nabla p_w - (\overline{\Lambda}\,gK\,\nabla h + \lambda_o K\,\nabla p_c) \tag{21}$$

To ease the model, we focus on water component with oil component as dependant. We then swap the expression consists of water pressure into right hand side as below.

$$-K\,\nabla p_w = \frac{1}{\lambda_T}(V_T + \overline{\Lambda}\,gK\,\nabla h + \lambda_o K\,\nabla p_c) \tag{22}$$

From equation (22), we than may define water velocity by substituting the right hand side term into water velocity equation.

$$V_w = \frac{\lambda_w}{\lambda_T}\left(-V_T + \overline{\Lambda} gK\nabla h + \lambda_o K\,\nabla p_c\right) - \lambda_w \rho_w gK\nabla h \tag{23}$$

Under two-phase flow condition, we have fractional flow as the ratio of fluid production rate over total production rate. Fractional flow according to the definition above shall be a value between 0 and 1. In the absence of gravity, in oil-water system, fractional flow for water taken from equation (18) and (19) can be denoted as

$$f_w = \frac{V_w}{V_w + V_o} \cong \frac{\lambda_w}{\lambda_T} \tag{24}$$

We now substitute water velocity in equation (23) with fractional flow terms and expand the term $\overline{\Lambda}$ into oil and water component.

$$V_w = f_w(-V_T + \lambda_o(\rho_w - \rho_o)gK\nabla h + \lambda_o K\,\nabla p_c) \tag{25}$$

Continuity equation in equation (5) above in this case is used to express velocity equation with saturation variable. Eliminating mass rates ρ in both sides of equation (5), we have:

$$\phi\frac{\partial S_w}{\partial t} + \frac{\partial v_w}{\partial x} = \frac{q_w}{\rho_w} \tag{26}$$

We then insert equation (24) into equation (25).

$$\phi\frac{\partial S_w}{\partial t} + \frac{\partial}{\partial x}[f_w(-V_T + \lambda_o(\rho_w - \rho_o)gK\nabla h + \lambda_o K\,\nabla p_c)] = \frac{q_w}{\rho_w} \tag{27}$$

Here we notice that pressure solver in equation (25) and updated saturation in equation (27) both are connected with variable of fractional flow through relative permeability.

The contact angle θ, which appears when a fluid interface intersects with a solid surface, is an important parameter to define the wetting phase and non-wetting phase.[8] To avoid excessive numerical analysis due to dissolved effect of fluid, we choose $\theta = 0$ for our scheme.

In this case, both equation (25) and (27) can be solved in sequence with a method called IMPES (Implicit Pressure, Explicit Saturation). This method will firstly solve pressure equation implicitly and then will solve saturation explicitly through velocity equation, which is previously derived from pressure solver. Under IMPES method, we notice that in equation (25) and (27), pressure of displaced fluid (oil pressure) and displacing fluid saturation (water saturation) are the primary unknowns we are solving. Some main variables like permeability and transmissibility in multi-phase flow are functions of these variables. Under IMPES, we define equation (27) in 2D areal flow as follows.

$$\phi \frac{\partial S}{\partial t} + \nabla.(f(S)V_T) = \frac{q}{\rho} \tag{28}$$

$$\phi \frac{\partial S}{\partial t} + a\frac{\partial f(S^n)}{\partial x} + b\frac{\partial f(S^n)}{\partial y} = \frac{q}{\rho} \tag{29}$$

a and b here represent wave speed which is the maximum absolute value of velocity.

$$f(S) = -\lambda(S)k\,\nabla u$$

$$a = \max\left|\lambda_{i+1/2,j}\left(\frac{u_{i+1,j} - u_{ij}}{\Delta x}\right)\right|$$

$$b = \max\left|\lambda_{i,j+1/2}\left(\frac{u_{i,j+1} - u_{ij}}{\Delta y}\right)\right|$$

This implies on requiring time step restriction known as CFL (Courant-Friedrichs-Levy) condition. With grid Δx, CFL number is given by:

$$CFL = \frac{|v_{max}|_{i,j}\,\Delta t}{\Delta x} \tag{30}$$

where v_{max} is the absolute maximum velocity within an element. To avoid the information extends one grid size per time step, the number is set as CFL < 1.

3.3. Discretising two-phase flow equations

As mentioned above, under two-phase flow there are two main solvers to be approximated. For pressure solver, we use the same equation with the one in single flow

[8] Source: [7]

scheme. The different is only that the permeability variable in two-phase flow is relative permeability $K\frac{k_{rw}}{\mu_w}$, which is a function of saturation derived from fractional flow. Modified from equation (8), under the system of two-phase flow, the equation for pressure solver for water phase is given below.

$$K\left[\frac{k_{rw}}{\mu_w}x_{i+\frac{1}{2},j}\right]\left[\frac{u_{i+1,j}}{\Delta x^2}-\frac{u_{i,j}}{\Delta x^2}\right]+K\left[\frac{k_{rw}}{\mu_w}x_{i-\frac{1}{2},j}\right]\left[\frac{u_{i-1,j}}{\Delta x^2}-\frac{u_{i,j}}{\Delta x^2}\right]$$
$$+K\left[\frac{k_{rw}}{\mu_w}y_{i,j+\frac{1}{2}}\right]\left[\frac{u_{i,j+1}}{\Delta y^2}-\frac{u_{i,j}}{\Delta y^2}\right]+K\left[\frac{k_{rw}}{\mu_w}y_{i,j-\frac{1}{2}}\right]\left[\frac{u_{i,j}}{\Delta y^2}-\frac{u_{i,j-1}}{\Delta y^2}\right]$$
$$=u_{i,j}^{n+1}-u_{i,j}^{n} \qquad (31)$$

From fractional flow term in equation (24), we have $f_w=\frac{q_w}{q_w+q_o}=\frac{\lambda_w}{\lambda_T}$. We may expand the equation into $f_w=\frac{k_{rw}/\mu_w}{k_{rw}/\mu_w+k_{ro}/\mu_o}$. The water flooding illustration above mentions that both $K_{rw}(S_w)$ and $K_{ro}(S_o)$ are functions of saturation which are updated through time step along with constant injection at sink point. The relative permeability for each phase in functional form, adopted from *Aziz and Settari* (*1979*) [1], is given below.

$$k_{rw}=k_{rw}^{o}\left(\frac{S_w-S_{wr}}{1-S_{wr}-S_{or}}\right)^{\beta w};\ S_{wr}\le S_w\le 1-S_{or} \qquad (32)$$

$$k_{ro}=k_{ro}^{o}\left(\frac{S_o-S_{or}}{1-S_{wr}-S_{or}}\right)^{\beta w};\ S_{or}\le S_o\le 1-S_{wr} \qquad (33)$$

Here, S_{or} and S_{wr} are residual saturation for oil and water phase. For simplicity in MATLAB® coding based on relative permeability graphic shown in figure (6), that permeability is optionally considered as quadratic functions of saturation. We then define mobility of fluid as follow.

$$\lambda_w=\frac{{S_w}^2}{\mu_w};\ \lambda_o=\frac{(1-S_w)^2}{\mu_o};\ S_w=\frac{{S^o}_w-S_{wr}}{1-S_{wr}-S_{or}} \qquad (34\text{ a. }34\text{ b. }34\text{ c})$$

Assuming there is no trapped oil and water, then adopted from [3], S_{or} and S_{wr} = 0.

From equation (27), in the right hand side, $\frac{q_w}{\rho_w}$ is the matrix of injected inlets and outlets. Therefore, it is 1 for outlets and -1 for inlets. In MATLAB®, we will have one

column matrix with one value of the elements represents an inlet or an outlet while the rest values are zero. The matrix defines the position of inlets and outlets within the grid-blocks. This allows the coding to automatically switch the matrix as the positions of source and sink change. In formational equation, the saturation solver is defined as follow.

$$S^{n+1} = S^n + \frac{\Delta t}{\phi}\left(q_{max} - \sum_{n+1}^{n}\left(f(S)\, v_{ij}\right) + q_{min}\right) \tag{35}$$

Where in formational equation, v_{ij} is denoted below.

$$\begin{aligned} v_{ij} = {} & \lambda x_{w\left(i+\frac{1}{2}\right),j}\ \frac{\Delta y_j}{\Delta x_{i+\frac{1}{2}}}\left(u_{w(i+1)} - u_{w(i)}\right) \\ & + \lambda x_{w\left(i-\frac{1}{2}\right),j}\ \frac{\Delta y_j}{\Delta x_{i+1/2}}\left(u_{w(i-1)} - u_{w(i)}\right) \\ & + \lambda y_{w\, i,\left(j+\frac{1}{2}\right)}\ \frac{\Delta x_i}{\Delta y_{j+\frac{1}{2}}}\left(u_{w\,(j+1)} - u_{w(j)}\right) \\ & + \lambda y_{w\, i,\left(j-\frac{1}{2}\right)}\ \frac{\Delta x_i}{\Delta y_{j+\frac{1}{2}}}\left(u_{w\,(j-1)} - u_{w(j)}\right) \end{aligned} \tag{36}$$

As a re-check, it can be seen in equation (35) that when $\Delta x \to 0$ and $\Delta t \to 0$, the equation will reduce to continuity equation. In the equation, $f(S)$ is fractional flow, v_{ij} is velocity matrix that represents cell volume transmissibility and q_{max} and q_{min} represent positive and negative parts of the element inside velocity matrix. Matrix v_{ij} in MATLAB® will be either a non-zero upper or a non-zero lower matrix, depends on the location of sink and source in matrix q. For the solver we also set the updated saturation to follow statements in equation (32) and equation (33) to be:

$$S_{wr} \leq S_i{}^{n+1} \leq 1 - S_{or} \tag{37}$$

In this case, equation (34 a – c) will be used twice. First, it will be the input to define relative permeability for solving the pressure. Second, the relative permeability values are also the input of fractional flow, which is the updating value in the right hand side of equation (35).

Here, with some matrix manipulation in MATLAB®, the fractional flow command contains saturation variable that is updated based on equation (36) within the

time step iteration. Typically, for oil-water system, the plot of fractional flow for water phase is as figured below.

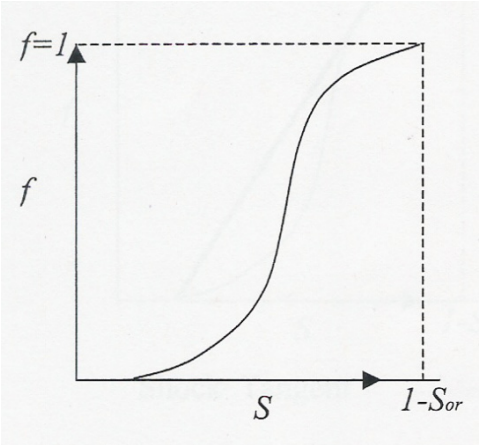

Figure 13. Fractional flow without gravity.[9]

In the right hand side of equation (35), as it is previously mentioned, Δt takes important part under IMPES method. The updating value for saturation S^{n+1} and stabilization of the loop calculation mainly depend on it. Details on its discretisation are available in [1]. From CFL condition in equation (30), we can derive in 2D that:

$$\Delta t = \frac{CFL}{\phi \, |v_{max}|_{ij}} \left(\frac{\Delta x}{u_x} + \frac{\Delta y}{u_y} \right) \leq 1 \qquad (38)$$

While Δt is between 0 and 1, CFL here has a function of breaking the iteration at Δt th while it keeps allowing the computation running for the next injection loop. The saturation matrix as the result is a square matrix. The value of each element is changing during the loop. The changing represents the changing of saturation itself due to constant influx.

[9] Source: [3]

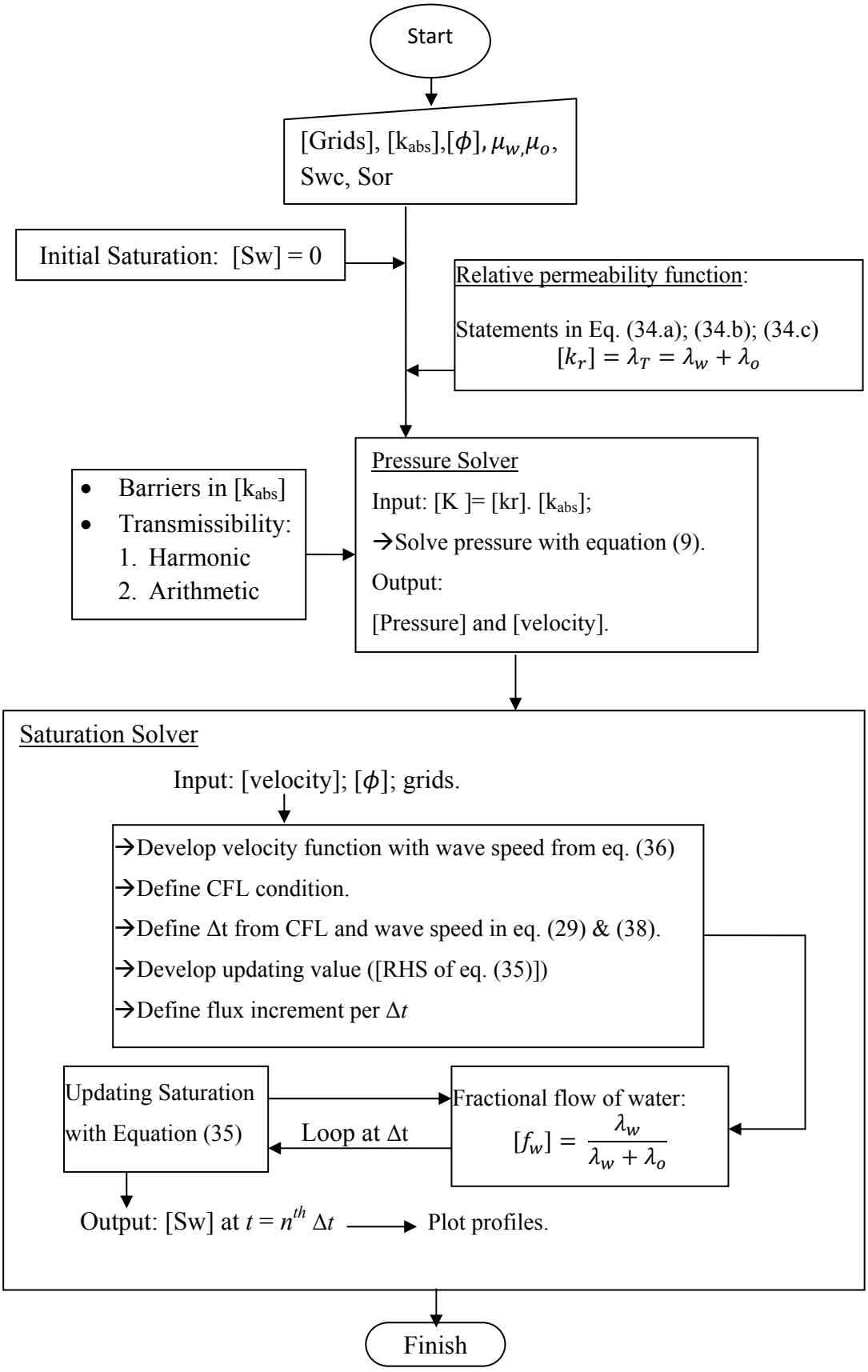

Figure 14. Flowchart of two-phase immiscible flow.

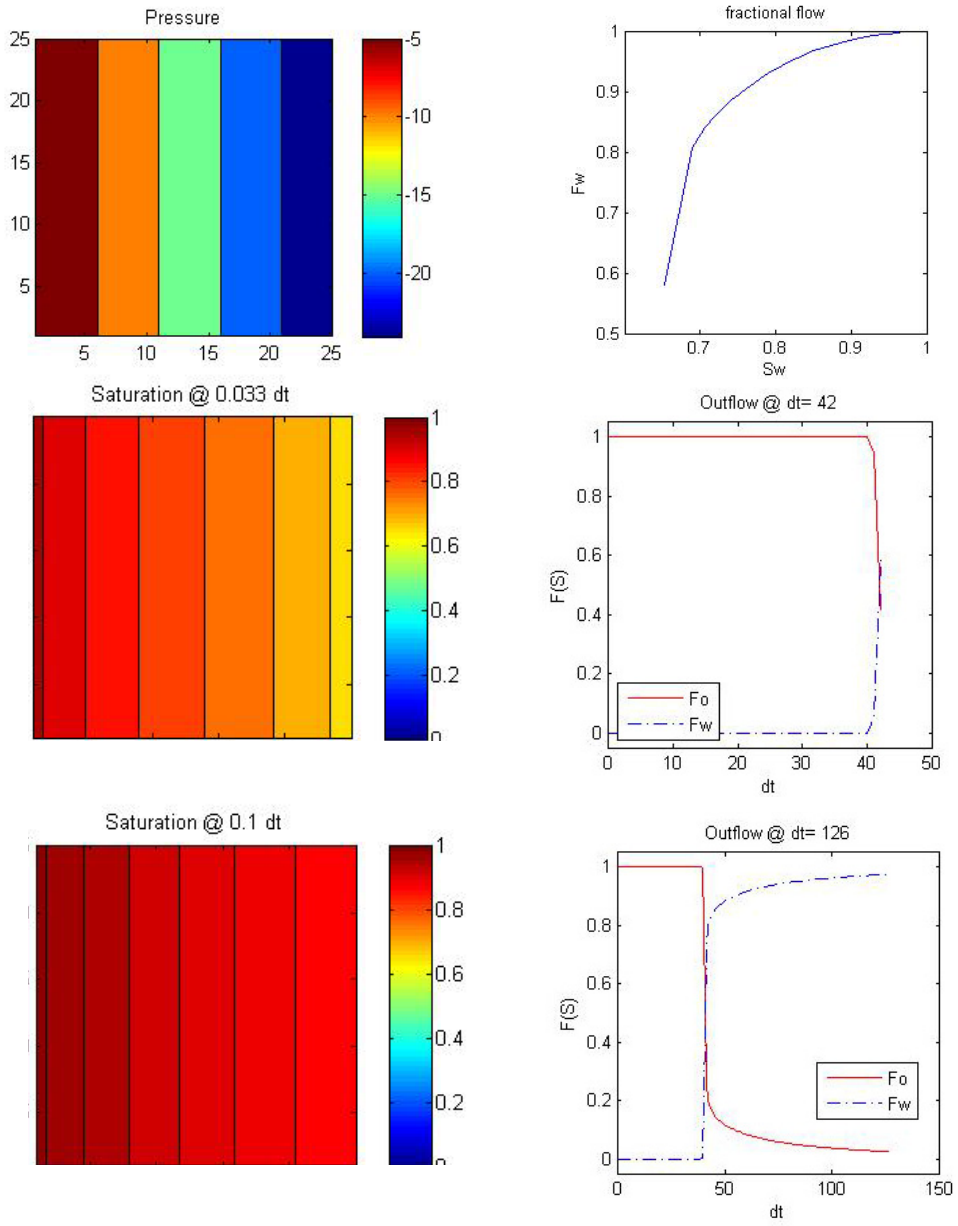

Figure 15. Profiles of pressure, fractional flow, saturation at different time steps, *Sw* at outlet and *Fo* (oil fractional flow) at outlet for a 1D square 25 grid-blocks.

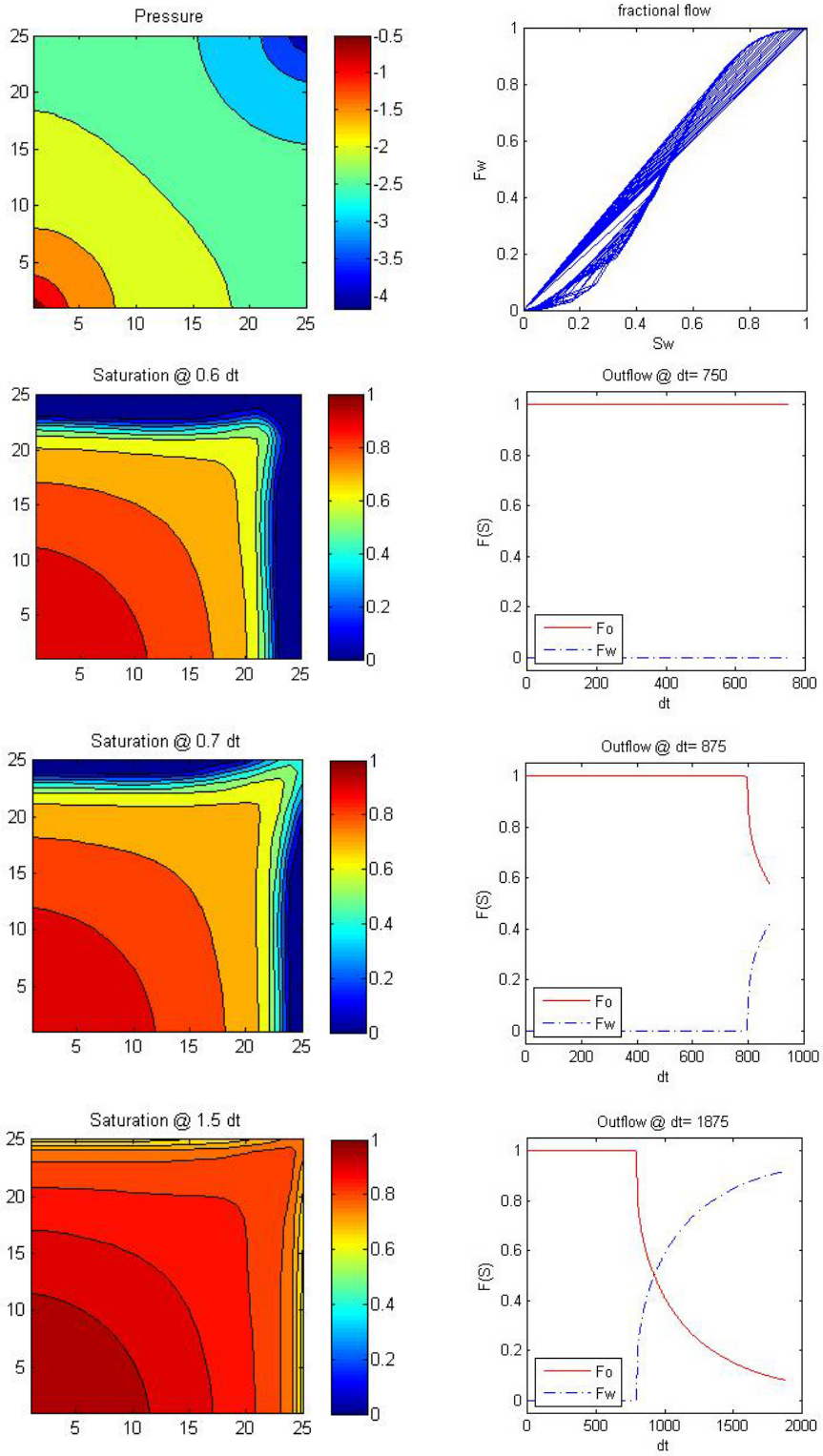

Figure 16. Profiles of pressure, fractional flow, saturation at different time steps, *Sw* at outlet and *Fo* (oil fractional flow) at outlet for a 2D square 25 grid-blocks.

3.4 Buckley-Leverett Equation

From the last description, we have defined the time when the breakthrough time occurs. We now will define the position of fluid front at time Δt^{th}. For this definition, Buckley-Leverett (1942) have in detail, discussed the descriptions in their paper. Taking from continuity equation in equation (5), we let ρ is constant and eliminated from both sides. v equals to phase fluid fractional volume $f(S)v$. In water formational equation, we denote as follows. We also let v in 1D form as total flux q_t

$$-\frac{\partial f(S_w)}{\partial x} = \frac{A\,\phi}{q_t}\frac{\partial S_w}{\partial t} \tag{39}$$

Fractional flow is normally a function of saturation in time Δt instead of a function of space Δx. To account with that, we have saturation variable as a function of space and time $S(x,\ t)$. Connecting the two conditions, we re-write equation (39) as follow.

$$-\frac{df(S_w)}{dS_w}\frac{\partial S_w}{\partial x} = \frac{A\,\phi}{q_t}\frac{\partial S_w}{\partial t} \tag{40}$$

For saturation change dS_w equals to zero during the displacement process, we denote the expression $S(x,\ t)$ below.

$$dS_w = \frac{\partial S_w}{\partial x}dx + \frac{\partial S_w}{\partial t}dt = 0 \tag{41}$$

The front location in time is derived from substituting expressions in equation (41) into equation (40). In this case the equation is denoted below.

$$\frac{\partial x}{\partial t} = \frac{q_t}{A\,\phi}\frac{df(S_w)}{dS_w} \tag{42}$$

3.5 Truncation Error

The approximation we are using is a finite numerical step approximation. The approximation inevitably leads us to some error. This error will still exist even if we use a better precision in our approximation. The error is explicable with Taylor series.

Using Taylor series method, let us consider constant time t + Δt in 1D space derivative. The pressure function is expanded as follows.

$$p(x+\Delta x, t+\Delta t) = p(x,t+\Delta t) + \Delta x \frac{\partial p}{\partial x}(x,t+\Delta t) + \frac{(\Delta x)^2}{2!}\frac{\partial^2 p}{\partial x^2}(x,t+\Delta t) + \frac{(\Delta x)^3}{3!}\frac{\partial^3 p}{\partial x^3}(x,t+\Delta t) + \cdots \quad (43)$$

$$p(x-\Delta x, t+\Delta t) = p(x,t+\Delta t) + (-\Delta x)\frac{\partial p}{\partial x}(x,t+\Delta t) + \frac{(-\Delta x)^2}{2!}\frac{\partial^2 p}{\partial x^2}(x,t+\Delta t) + \frac{(-\Delta x)^3}{3!}\frac{\partial^3 p}{\partial x^3}(x,t+\Delta t) + \cdots \quad (44)$$

We then add the two equations and solve the second derivative as follow.

$$\frac{\partial^2 p}{\partial x^2}(x,t+\Delta t) = \frac{p(x+\Delta x,t+\Delta t) - 2p(x,t+\Delta t) + p(x-\Delta x,t+\Delta t)}{(\Delta x)^2} + \frac{(\Delta x)^2}{12}\frac{\partial^4 x}{\partial x^4}(x,t+\Delta t) + \cdots \quad (45)$$

Under grid system, we can rewrite the equation into:

$$\left(\frac{\partial^2 p}{\partial x^2}\right)_i^{t+\Delta t} = \frac{p_{i+1}^{t+\Delta t} - 2p_i^{t+\Delta t} + p_{i-1}^{t+\Delta t}}{(\Delta x)^2} + h.o.t \quad (46)$$

$$h.o.t \sim higher\ order\ terms$$

Under constant x, we can then define the error in 1D time derivative using the same Taylor series method. From saturation solver, we have:

$$\frac{S(x,t)-S(x,t+\Delta t)}{\Delta t}+\frac{a}{\Delta x}\big(S(x,t)-S(x-\Delta x,t)\big)=0 \tag{47}$$

In Taylor series, we can write the first and second term of the equation into:

$$\frac{S(x,t+\Delta t)-S(x,t)}{\Delta t}=\frac{\partial S}{\partial t}(x,t)+\frac{\Delta t}{2}\frac{\partial^2 S}{\partial t^2}(x,t)+\frac{(\Delta t)^2}{3!}\frac{\partial^3 S}{\partial t^3}(x,t)+\cdots \tag{48}$$

$$\frac{S(x,t)-S(x-\Delta x,t)}{\Delta x}=\frac{\partial S}{\partial x}(x,t)+\frac{\Delta x}{2}\frac{\partial^2 S}{\partial x^2}(x,t)+\frac{(\Delta x)^2}{3!}\frac{\partial^3 S}{\partial x^3}(x,t)+\cdots \tag{49}$$

Adding the two equations, we have the truncation error from eliminating the first derivatives in both equations as follow.

$$\frac{1}{2}\left(\Delta t\frac{\partial^2 S}{\partial t^2}-a\,\Delta x\frac{\partial^2 S}{\partial x^2}\right)+h.o.t \tag{50}$$

Here we notice that the truncation error based on space is second order derivation while the error in time derivation is first order expression.

For $\frac{\partial S}{\partial t}+a\frac{\partial S}{\partial X}=0$, we may also write it into second derivative as follow.

$$\frac{\partial^2 S}{\partial t^2}=a^2\,\frac{\partial^2 S}{\partial x^2} \tag{51}$$

Substituting the term in equation (51) into equation (50), we obtain an equation below.

$$\frac{\partial^2 S}{\partial t^2}=\frac{(\Delta t\,a^2-a\,\Delta x)}{2}\frac{\partial^2 S}{\partial x^2} \tag{52}$$

$$\frac{\partial^2 S}{\partial t^2}=\frac{a\,\Delta x}{2}\left(\frac{a\,\Delta t}{\Delta x}-1\right)\frac{\partial^2 S}{\partial x^2} \tag{53}$$

Let $v=\frac{a\,\Delta t}{\Delta x}$ which represents CFL number. In full formational form, combining the expression in equation (53) into $\frac{\partial S}{\partial t}+a\frac{\partial S}{\partial X}=0$, we obtain an equation below.

$$\frac{\partial S}{\partial t}+a\frac{\partial S}{\partial x}=\frac{a\,\Delta x}{2}(1-v)\frac{\partial^2 S}{\partial x^2}+O(\Delta x^2) \tag{54}$$

We also notice that the coefficient term in the right hand side represents CFL restriction. The equation explains why CFL is set less than or equal to one.

3.6 Barriers in permeability matrix.

We also present other attempts in varying the permeability matrix. Our next attempt is to set square flow barrier in the middle of the reservoir. The second attempt is to set two symmetric rectangular flow barriers. Both of them are figured below.

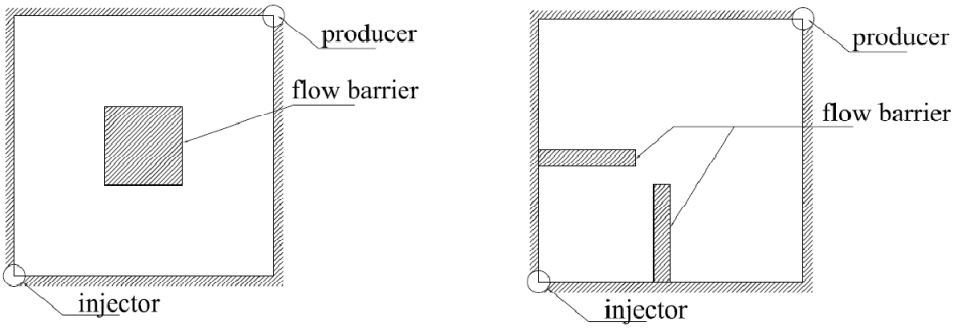

Figure 17. Variational models with flow barriers. (a). square barrier in the middle. (b). symmetrical rectangular barriers in the corner.

To account the first attempt, in MATLAB, we set the barrier for 10 by 10 grid blocks reservoir as follow.

$$k(i, j) = 1,$$
$$[(4 \leq i \leq 7) \text{ and } (4 \leq j \leq 7)] \rightarrow k = 0.001$$

From this attempt, we expect the flow to avoid the barrier in the middle. We also present the saturation profile with the existence of this type of barrier. Similar to the first attempt, the second attempt for 10 by 10 grid blocks barrier conditions in MATLAB will be denoted below.

$$k(i, j) = 1,$$
$$[(i = 6) \text{ and } j < 5\ ] \rightarrow k = 0.001$$
$$[(j = 6) \text{ and } i < 5\ ] \rightarrow k = 0.001$$

For the second attempt, in particularly, we will also try to set the transmissibility as arithmetic means to compare with the one with harmonic means.

To approach heterogenic physical condition of reservoir, we also set an attempt where permeability matrix exists as random number between 0 and 1000. Below, we also present flow profiles for 17 by 17-2D grid-block with random value permeability and rectangular barriers. We expect to visualize reservoir as mixed of rock and sand with different permeability. The graphical outputs also show clearly of trapped oil.

Some spots in the reservoir are not completely swept out by the water flooding. This matter leads to reservoir management to establish the best location arrangement of inlets and outlets in order to maximize the oil production.

3.7 Discussion

Outputs in figure 15 show that in homogenous 2D areal model, during first injection, water will reach the last grid block at $0.6 < CFL < 0.7$. This condition known as breakthrough, in which injected water has fulfilled approximately 0.6 - 0.7 part of pore volume of the reservoir.

With normal harmonic mean (figure 19), we can figure that the flow with this type of barrier would not flow through the barrier. This leads to the decrease of breakthrough time. The breakthrough time reduces as the arrangement of the barriers prevents the flow to flood the whole block and drives it to the outlet more quickly. However, with arithmetic mean (figure 20), we notice that the flow pass through the barrier which actually means a wrong approximation. The arithmetic average transmissibility allows the flow to pass through the boundary in a parallel way. This explains why the flow profile under arithmetic average with 2^{nd} type of barrier is similar to the flow under homogenous grids without barrier.

In 1D homogenous system, the piston-like movement of water-oil displacement is more obvious. The figures for the movement against time are as figured in figure 15. This happens due to immiscible system that does not consider solubility. The neglecting of solubility is a result from previous empirical observations. In the figure, we can also notice that the pushing movement leads to straight line in outflow profiles. This means that before breakthrough occurs, the outlet is producing oil that is free from water.

In 2D fractional flow graphic profile, we notice that when the iteration is closing to breakthrough time (finger-like profile saturation) or when oil saturation increases rapidly, the graphic line is shifting on right movement. In some literatures ([8] and [9]), the condition means as efficient displacement when mobility ratio is very low or when oil viscosity is very low. The effect of mobility ratio is one factor in enhanced oil recovery (EOR). A glance review, according to the literatures, the primary recovery is carried out by existing natural pressure inside reservoir as an effect of the existence of trapped fluid inside reservoir. To maintain the pressure level, water or gas is injected. The quarter five spot water-oil system that we model is the secondary recovery.

The logic of lowering mobility ratio is that we try to optimize the oil production with efficient water-flooding process. If mobility ratio is too high, it means water mobility is higher than that of the oil. When water mobility is high, water viscosity is low and water tends to run avoiding oil. This condition will create a fingering profile of water through oil instead of pushing the oil constantly as piston-like movement. Mobility ratio matters more when we deal with random heterogenic reservoir. Further details on enhanced oil recovery process and the involved factors are available in [8] and [9].

As a comparison for our result in this thesis, in the end of our first section above, we present a review of the applicability of mixed-FEM for pressure solver. The approximation is based on standard mixed finite element where it solves pressure and velocity in one-step solution. Other results for two-phase flow using higher order finite element based on IMPES are presented in [13] and [14]. Both papers discuss higher-order finite element implementation for convective flux approximation in more detail. The implementation is presented into comparison manner between CVFE and control volume distributed (CVD) for approximating the flux in two-phase flow on unstructured grids for water-oil system in 2D simulation ([13]) and 3D simulation ([14]). A glance review, the papers emphasize the benefit of control volume distributed to improve fluid front resolution on unstructured grids both in 2D and 3D two-phase flow.

We also notice error due to the approximation based on grid-block. A simple numerical dispersion illustration in figure 10 shows basic error of the approximation. From the illustration, we can simply guess that water will reach the last block when the iteration number equals to the number of the grid with less rate due to the permeability. The more the number of grid, the longer water reaches the last block. Based on Buckley-Leverett equations, we can define the fluid front position, which we cannot achieve in our model due to grid block system with Δx. In other words, our grid model converts x-location into grid-block position. This error, indeed, will be reduced when we apply finer grid for the same length to approach the real condition. As we mentioned above, some simplicities are applied in generating our model. Simplicities that may apply in a real approximation for reservoir appraisal in the early stage, also contribute error in the approximation. However, this type of error will be improved gradually while recovery process is running.

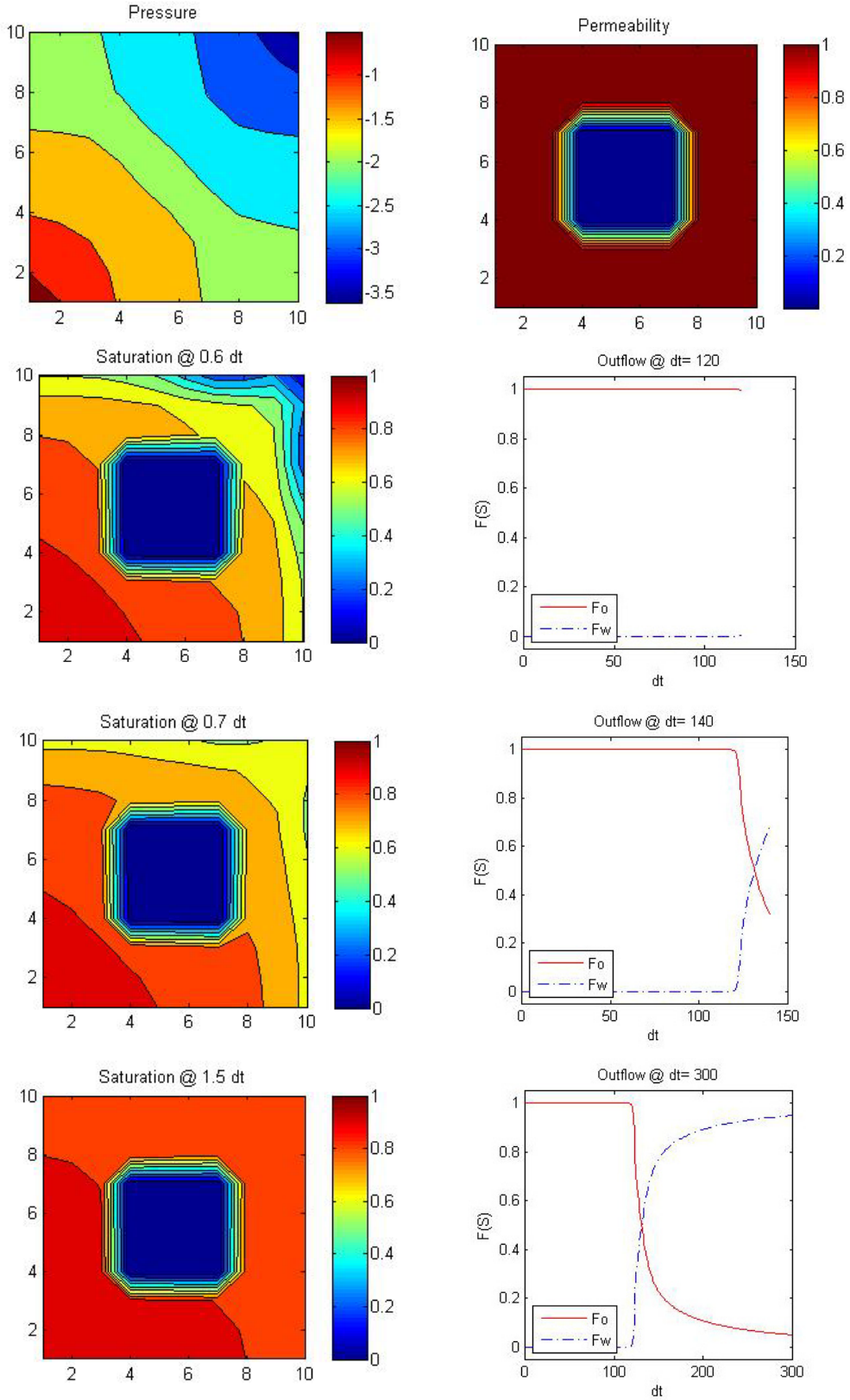

Figure 18. Profiles of pressure, fractional flow, saturation at different time steps, Sw at outlet and Fo (oil fractional flow) at outlet for a square 10 grid-blocks with barrier type 1.

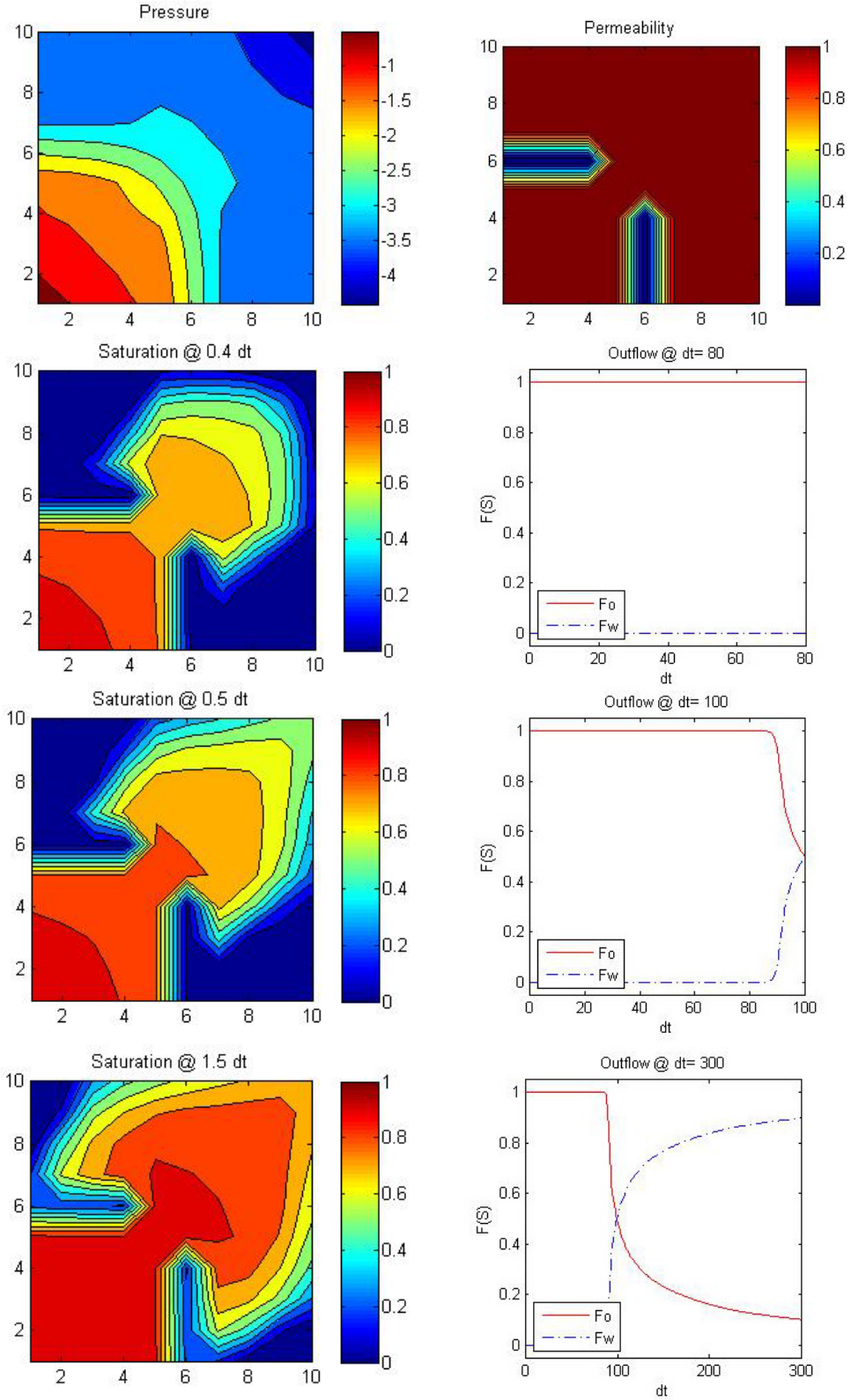

Figure 19. Profiles of pressure, fractional flow, saturation at different time steps, *Sw* at outlet and *Fo* (oil fractional flow) at outlet for a square 10 grid-blocks with barrier type 2 running with harmonic mean.

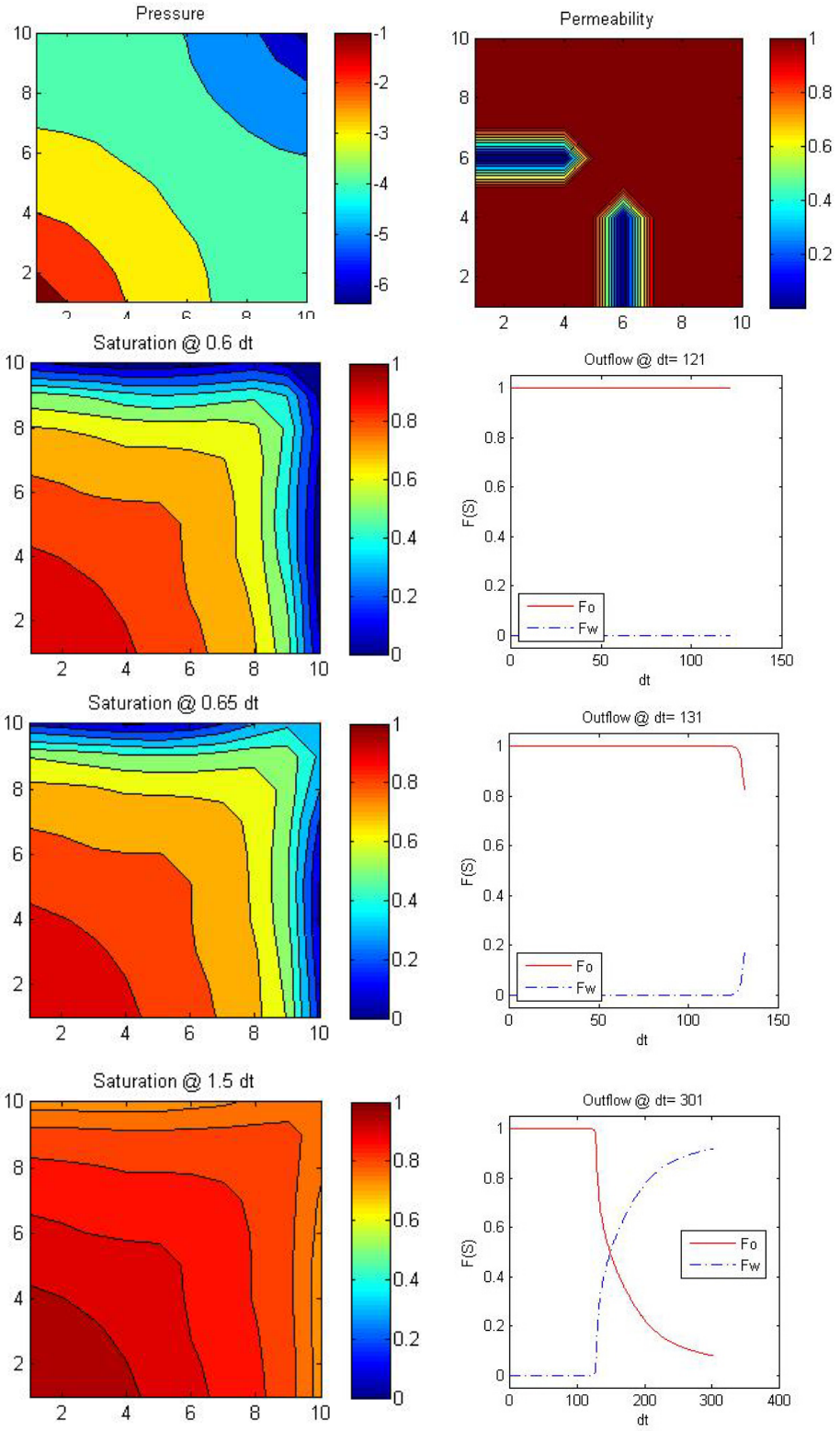

Figure 20. Profiles of pressure, fractional flow, saturation at different time steps, *Sw* at outlet and *Fo* (oil fractional flow) at outlet for a square 10 grid-blocks with barrier type 2 running with arithmetic mean.

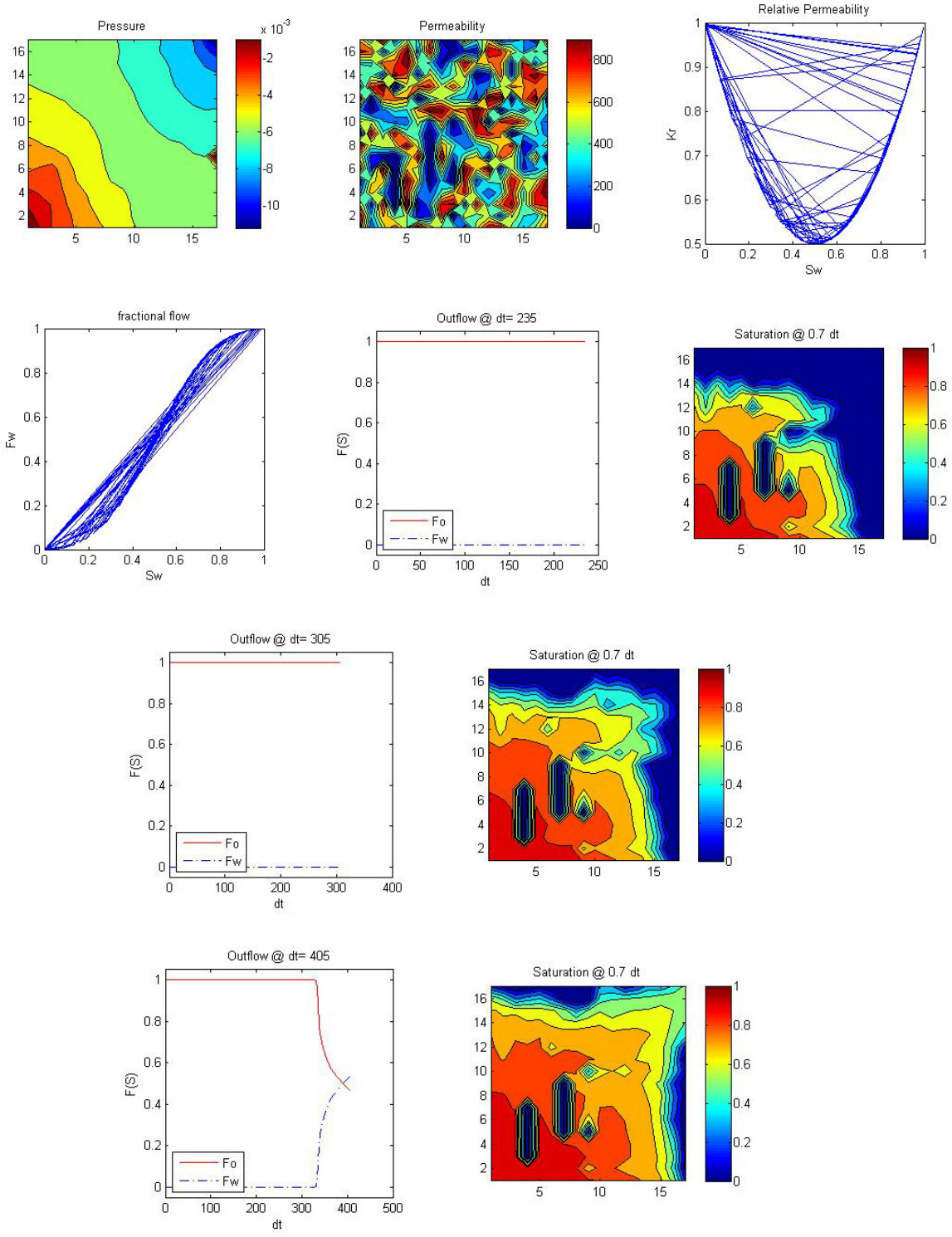

Figure 21. Profiles of pressure, fractional flow, saturation at different time steps, *Sw* at outlet and *Fo* (oil fractional flow) at outlet for a square 17 grid-blocks with random permeability and rectangular barriers.

A1 Appendix A

Appendix A

Single flow MATLAB® coding:

```
clear all; clc
nblox=14; nbloy=14;
ngrid=nblox*nbloy;
k=ones(nblox,nbloy);mu=1;L=k./mu;
dx=1/nbloy.*ones(nblox,nbloy-1);dy=1/nblox.*ones(nblox-1,nbloy);
tx=.5*dx./k(:,1:nbloy-1);txi=.5*dx./k(:,2:nbloy);
ty=.5*dy./k(1:nblox-1,:);tyi=.5*dy./k(2:nblox,:);
Tx=dx./(tx+txi);Tx=(dy(1)./dx(1)).*Tx;
Ty=dy./(ty+tyi);Ty=(dx(1)./dy(1)).*Ty;Ty(nblox,:)=0;
T=sparse(1:ngrid-1,2:ngrid,Ty(1:ngrid-1),ngrid,ngrid);
T=-T-sparse(2:ngrid,1:ngrid-1,Ty(1:ngrid-1),ngrid,ngrid);
T=T-sparse(1:ngrid-nblox,nblox+1:ngrid,Tx,ngrid,ngrid);
T=T-sparse(nblox+1:ngrid,1:ngrid-nblox,Tx,ngrid,ngrid);
diagT=spdiags(T); diagv=(abs(sum(diagT,2)));
A=T+sparse(1:ngrid,1:ngrid,diagv,ngrid,ngrid);
A(1,1)=A(1,1)+sum(k(:,1))+sum(k(1,:));          % prescribing pressure (1,1) = 0
 Q([1 ngrid])=[-1 1];                           % for 2D system
% Q(1:nblox)=1;Q(ngrid-nblox+1:ngrid)=-1;       % for 1D system
u=A^-1*Q';
p=reshape(u,nblox,nbloy);
tri=Ty(1:nblox-1,:);
trj=Tx(:,1:nbloy-1);
Vx=(p(1:nblox-1,:)-p(2:nblox,:)).*tri;
Vy=(p(:,1:nbloy-1)-p(:,2:nbloy)).*trj;
subplot(2,2,1);contourf(p),colorbar;grid on,title('Pressure');
[x,y]=meshgrid(1:nblox,1:nbloy);
[xa,xb]=gradient(p,.2,.2);
[za,zb]=meshgrid(1:nblox,1:nbloy);
subplot(2,2,2),streamline(x,y,xa,xb,za,zb);grid on,title('Streamline flow');
subplot(2,2,3),surf(p),colorbar;
subplot(2,2,4),quiver(x,y,xa,xb);
```

A2 Appendix B

Appendix B

Two-Phase Flow MATLAB® coding

```
clear all; clc;clf;
nblox=10; nbloy=10;
ngrid=nblox*nbloy;
%  options for permeability
k=ones(nblox,nbloy);                        %  uniform permeability
% k(4:7,4:7)=.00001;                        %  perm. with square barrier
% k(1:4,6)=.00001;k(6,1:4)=.00001;          %  perm. with symmetric rect. barriers
% k=randi([0,1000],nblox,nbloy);            %  random permeability
L=k;
trans=1;                                    % 1 --> harmonic; 2 --> arithmetic
dx=1/nbloy.*ones(nblox,nbloy-1);dy=1/nblox.*ones(nblox-1,nbloy);
por=ones(nblox,nbloy);
system=2;                                    % 1 --> 1D; 2 --> 2D
disp([num2str(system),'D system']);
if system==1;
   Q(1:nblox)=1;Q(ngrid-nblox+1:ngrid)=-1;
else
   if system==2;
   Q([1 ngrid])=[1 -1];end;
end
muw=1; muo=1;
swc=0; sor=0;
S=zeros(ngrid,1);
CFL=0.7;                                    %  0 – 1 (for single flooding)
[p,Vx,Vy]=Pressure(nblox,nbloy,ngrid,L,dx,dy,trans,S,muw,muo,swc,sor,Q);
sat(nblox,nbloy,ngrid,por,Vx,Vy,muw,muo,swc,sor,Q,S,CFL);
subplot(2,3,1),contourf(p),title('Pressure'),axis square;colorbar;
subplot(2,3,2),contourf(k),title('Permeability'),axis square; colorbar;
```

Relative Permeability Function

```
function [Lw,Lo,Fw]=relperm(S,muw,muo,swc,sor)
S = (S-swc)/(1-swc-sor);
Lw = S.^2/muw;              % Water mobility
Lo =(1-S).^2/muo;           % Oil mobility
Fw=Lw./(Lw+Lo);             % water fractional flow
```

Pressure Solver

```
function [p,Vx,Vy]=Pressure(nblox,nbloy,ngrid,L,dx,dy,...
   trans,S,muw,muo,swc,sor,Q)
[Lw,Lo]=relperm(S,muw,muo,swc,sor);
Lt=Lw+Lo;Lt=reshape(Lt,nblox,nbloy);Lt=Lt.*L;
if trans==1
% harmonic mean
tx=.5*dx./Lt(:,1:nbloy-1);txi=.5*dx./Lt(:,2:nbloy);
ty=.5*dy./Lt(1:nblox-1,:);tyi=.5*dy./Lt(2:nblox,:);
Tx=dx./(tx+txi);Tx=(dy(1)./dx(1)).*Tx;
Ty=dy./(ty+tyi);Ty=(dx(1)./dy(1)).*Ty;Ty(nblox,:)=0;
else
   if trans==2
% arithmetic mean
tx=.5*dx.*Lt(:,1:nbloy-1);txi=.5*dx.*Lt(:,2:nbloy);
ty=.5*dy.*Lt(1:nblox-1,:);tyi=.5*dy.*Lt(2:nblox,:);
Tx=(tx+txi)./(2*dx);Tx=(dy(1)./dx(1)).*Tx;
Ty=(ty+tyi)./(2*dy);Ty=(dx(1)./dy(1)).*Ty;Ty(nblox,:)=0;
   end
end
T=sparse(1:ngrid-1,2:ngrid,Ty(1:ngrid-1),ngrid,ngrid);
T=-T-sparse(2:ngrid,1:ngrid-1,Ty(1:ngrid-1),ngrid,ngrid);
T=T-sparse(1:ngrid-nblox,nblox+1:ngrid,Tx,ngrid,ngrid);
T=T-sparse(nblox+1:ngrid,1:ngrid-nblox,Tx,ngrid,ngrid);
diagT=spdiags(T); diagv=(abs(sum(diagT,2)));
A=T+sparse(1:ngrid,1:ngrid,diagv,ngrid,ngrid);
A(1,1)=A(1,1)+sum(Lt(:,1))+sum(Lt(1,:));
u=A^-1*Q';
p=reshape(u,nblox,nbloy);
tri=Ty(1:nblox-1,:);
trj=Tx(:,1:nbloy-1);
Vx=(p(1:nblox-1,:)-p(2:nblox,:)).*tri;
Vy=(p(:,1:nbloy-1)-p(:,2:nbloy)).*trj;
```

Saturation Solver

```
function sat(nblox,nbloy,ngrid,por,Vx,Vy,muw,muo,swc,sor,Q,S,CFL)
%  Storing positive and negative velocity into matrix
maxvx(2:nbloy,:)=max(Vx,0);
maxvy(:,2:nblox)=max(Vy,0);
minvx=min(Vx,0); minvx(nblox,:)=0;
minvy=min(Vy,0); minvy(:,nbloy)=0;
vt=maxvx-minvx+maxvy-minvy; vt=reshape(vt,ngrid,1);
qmax=max(Q,0); qmin=min(Q,0);
volc=1/ngrid; porv=volc.*por;
porv=reshape(porv,ngrid,1);                    % pore volume
ws=min(porv./(vt(:)+qmax')); hws=ws/2;         % wave speed
dt=ceil(CFL/hws);                              % 2nd R.H.S of the equation
inc=(CFL./dt)./porv;                           % updating value per injection
v=abs(sparse(1:ngrid-1,2:ngrid,minvx(1:ngrid-1),ngrid,ngrid));
v=abs(v-sparse(2:ngrid,1:ngrid-1,maxvx(2:ngrid),ngrid,ngrid));
v=abs(v-sparse(1:ngrid-nblox,nblox+1:ngrid,minvy(1:ngrid-nblox),ngrid,ngrid));
v=abs(v-sparse(nblox+1:ngrid,1:ngrid-nblox,maxvy(nbloy+1:ngrid),ngrid,ngrid));
diagvt=spdiags(v); diagv=-abs(sum(diagvt,2)+qmin');
Av=v+sparse(1:ngrid,1:ngrid,diagv,ngrid,ngrid);
Av=spdiags(inc,0,ngrid,ngrid)*Av;              % right hand side updating value
q=qmax'.*inc;                                  % influx updating value
for i=1:dt
   disp(['dt: ',num2str(i)]);
   [Lo,Lw,Fw]=relperm(S,muw,muo,swc,sor);
   if(max(Fw)>1),break;end
   S=S+(Av*Fw+q);                              % updating saturation
   if(max(S)>1),break;end
   sx=reshape(S,nblox,nbloy);
   fwi(i)=Fw(ngrid); si(i)=S(ngrid);
   subplot(2,3,3),plot(S,Lo+Lw),title('Relative Permeability'),...
      xlabel('Sw'),ylabel('Kr'),axis square;drawnow
   subplot(2,3,4),plot(S,Fw),title('fractional flow'),...
      xlabel('Sw'),ylabel('Fw'),axis square;drawnow
   subplot(2,3,5),ax=linspace(0,i,i);plot(ax,1-fwi,'r',ax,fwi,'-.b'),...
      title(['Outflow @ dt= ', num2str(i)]),xlabel('dt'),...
      ylabel('F(S)'),ylim([-0.05 1.05]),axis square;...
      legend('Fo','Fw',3);drawnow
   subplot(2,3,6),contourf(sx);title(['Saturation @ ',...
      num2str(CFL),' dt']),axis square;caxis([0 1]),colorbar,drawnow;
end
```

B Bibliography

Bibliography

1. Aziz, K. and Settari, A. Petroleum Reservoir Simulation. Applied Science Publishers Ltd, London 1979.
2. Fanchi, John R. Principles of Applied Reservoir Simulation. Gulf Professional Publishing, Houston-Texas 2001.
3. Edwards, M G. *Hand-out note*s. EGIM-27 Reservoir Modelling 2009. School of Engineering, University of Wales-Swansea 2009.
4. Abou-Kaseem, J H. Farouq Ali, S M. and Islam, Rafiq M. Petroleum Reservoir Simulation: A Basic Approach. Gulf Publishing Company, Houston-Texas 2006.
5. Peaceman, Donald W. Fundamentals of Numerical Reservoir Simulation. Elsevier Scientific Publishing Company, Amsterdam 1977.
6. Cao, Y. Eikemo, B. Helmig, R. Non-linearities and upscaling in porous media. Fractional Flow Formulation for Two-phase Flow in Porous media. International Research Training Group GRK1398/1. Universität Stuttgart 2007.
7. Faigle, B. Non-linearities and upscaling in porous media. Two-phase flow modeling in porous media with kinetic interphase mass transfer processes in fractures. International Research Training Group-NUPUS. Universität Stuttgart 2009.
8. Satter, A. Iqbal, G M. and Buchwalter, J L. Practical Enhanced Reservoir Engineering: Assisted with Simulation Software. PennWell Corporation, Tulsa, Oklahoma 2007.
9. Donaldson, E C. Chilingarian, G V. Yen, T F. Enhanced Oil Recovery II. Fundamentals and Analyses. Elsevier Science Publishers B.V. Elsevier Science Publishing Company Inc. New York 1985
10. Bahriawati, C. Carstensen, C. 3 MATLAB® Implementations of the Lowest-Order Raviart-Thomas MFEM with A Posteriori Error Control. Computational Methods In Applied Mathematics, Vol.5 (2005), No.4, pp.333-361© 2005 Institute of Mathematics of the National Academy of Sciences of Belarus.

11. Chen, Z. and Ewing, Richard E. From Single-Phase to Compositional Flow: Applicability of Mixed Finite Elements. Transport in Porous Media 27**:** 225–242, © Kluwer Academic Publishers. Netherlands 1997.
12. Wriggers, P. Carstensen, C. Finite Element Technologies. CISM Courses and Lectures, vol.509. SpringerWien. New York 2009.
13. Edwards M G **"**Higher-Resolution Hyperbolic - Coupled - Elliptic Flux-Continuous CVD Schemes on Structured and Unstructured Grids in 3-D". *Int. J. Numer Meth, Fluids 51 1079-1095, 2006*
14. Edwards M G **"**Higher-Resolution Hyperbolic - Coupled - Elliptic Flux-Continuous CVD Schemes on Structured and Unstructured Grids in 2-D". *Int. J. Numer Meth, Fluids 51 1059-1077, 2006*
15. Hahn, Brian D. Essential MATLAB® for Scientists and Engineers. Elsevier Butterworth-Heinemann. Oxford 2002.